DEPARTMENT OF THE ARMY CORPS OF ENGINEERS

BEACH EROSION BOARD
OFFICE OF THE CHIEF OF ENGINEERS

MODIFICATION OF THE QUADRATIC BOTTOM-STRESS LAW FOR TURBULENT CHANNEL FLOW IN THE PRESENCE OF SURFACE WIND-STRESS

TECHNICAL MEMORANDUM NO. 93

MODIFICATION OF THE QUADRATIC BOTTOM-STRESS LAW FOR TURBULENT CHANNEL FLOW IN THE PRESENCE OF SURFACE WIND-STRESS

TECHNICAL MEMORANDUM NO. 93
BEACH EROSION BOARD
CORPS OF ENGINEERS

FEBRUARY 1957

FOREWORD

High water and waves accompanying storms of hurricane intensity have periodically caused great damage along the Atlantic and Gulf coasts of the United States. Damage figures have risen with each succeeding great storm as more and more development of the shore areas has been made, reaching, for example, an estimated 200 million dollars in the Narragansett Bay area (including Providence, Rhode Island) for the 1954 hurricane Carol. Adequate, and economic, design of shore structures to prevent or mitigate this damage requires accurate prediction of water levels for possible future storms. Complete understanding of the development of storm surges along an open coast has not yet been realized although considerable progress in gaining a workable understanding is now being made. One of the factors involved in such computations is the effect of bottom roughness and the resultant bottom shear stress on the flow of water into and through an estuary, and consequently the final water elevation around the shores of the estuary due to hurricane surge and/or associated wind set-up. The steady state case, with zero mean flow in this report, is treated as a special case of the general theory, and the ratio between bottom stress and surface stress is found to depend upon the ratio of depth to bottom roughness, and is generally less than about 0.1.

The report was prepared at the Agricultural and Mechanical College of Texas by Robert O. Reid, an Associate Professor at that institution, in pursuance of contracts between the Texas A&M Research Foundation and the Beach Erosion Board (contract DA-49-055-Civ-eng-56-4) and the U. S. Weather Bureau (contract Cwb-8717). The work has been sponsored by the Corps of Engineers and the Weather Bureau as a part of their responsibilities in hurricane damage prevention, warning, and prediction, as outlined in Public Law 71, 84th Congress and Public Law 657, 80th Congress. The funds supplied by the Corps of Engineers were supplied through the New England Division as a part of a comprehensive study of hurricane prevention for the southern New England shore. The funds supplied by the Weather Bureau were from increased appropriations made for severe storm research during fiscal year 1956.

This report is published under authority of Public Law 166, 79th Congress, approved July 31, 1945.

TABLE OF CONTENTS

LIST OF SYMBOLS

B_o	parameter which depends upon m and r_o (eq 11)
B_1	parameter which depends upon m and r_1 (eq 11)
D	depth of channel
f_1	function of m defined for negative m only
f_2	function of m defined for positive m only
g	acceleration of gravity
G	a correction term in the fitted formula for m; depends upon α only
k_o	the von Karman dimensionless constant, 0.40
k_o'	$k_o(1 + r_o + r_1)$, very nearly equal to k_o
ln	$\log_e$
L	mixing length
L_o	mixing length at the rough bottom
L_1	mixing length at the free surface
m	ratio of τ_s to τ_b with appropriate sign
m_o	absolute value of m for the case of equilibrium set-up in a bounded channel
n	Manning's n (units of $[L]^{1/6}$), an empirical channel bed roughness parameter
r_o	ratio of Z_o to D, a very small quantity
r_1	ratio of Z_1 to D, a very small quantity
s	surface slope
u	temporal mean velocity at level z in the x direction
u_s	temporal mean velocity at the surface
U	relative velocity $u/\sqrt{\lvert\tau_s\rvert/\rho}$
U_a	U at $\zeta < \zeta_m$ for the case of negative m
U_b	U at $\zeta > \zeta_m$ for the case of negative m
U_m	U at $\zeta = \zeta_m$ (maximum relative velocity for the case of negative m)
U_s	relative surface current
v	mean current, averaged over the entire depth of the channel
v*	$\pm\sqrt{\lvert\tau_s\rvert/\rho}$ where the sign is taken consistent with that of τ_s

V	relative mean current v/v^*
V'	V as defined by the asymptotic relation (42)
V_o	value of V for the case of $m = 0$ depends upon D/Z_o (or γ_b)
V_1	value of V for the case of $m = 1$, depends upon D/Z_o (or γ_b)
W	surface of wind speed
y	dimensionless variable which depends upon ζ and m (eq 11)
z	elevation above bottom (distance from the boundary)
z_o	characteristic roughness length for the bottom
z_1	characteristic roughness length for the free surface
α	a dimensionless parameter in the fitted formula for m.
γ_b	non-dimensional proportionality factor which depends upon bottom roughness and channel dimensions
ζ	dimensionless elevation Z/D
ζ_m	value of ζ at the position of maximum subsurface current for the case of negative m
ρ	density of the water
τ	shear stress (force per unit area) exerted at level z by the upper fluid on the fluid below this level
τ_b	shear stress exerted on the bottom by the water
τ_s	shear stress exerted by the air on the upper surface of the water

MODIFICATION OF THE QUADRATIC BOTTOM-STRESS LAW FOR TURBULENT CHANNEL FLOW IN THE PRESENCE OF SURFACE WIND-STRESS

by

R. O. Reid
Associate Professor of Oceanography
A&M College of Texas

ABSTRACT

The simple quadratic formula for stream bed resistance is inadequate when an appreciable wind stress exists at the surface of the stream. In the present paper a generalized formula for velocity profile and bottom stress is derived which takes the influence of surface stress into account. The theory applies to quasi-steady flow over a hydrodynamically rough stream bed and makes use of Montgomery's (1943) generalization of the Prandtl-von Karman mixing length theory, where both stress and mixing length are continuous functions of elevation, from the stream bed to the surface. The simple quadratic law (eq. 1) is a special case of the general formula for bottom stress (eqs.(40a,b) and (41a,b), or (43) through (45)), and represents in effect an asymptotic form which applies when the mean stream velocity is very large relative to the surface stress. The bed resistance coefficient γ_b^2 (eq. (30)) is a characteristic parameter of the general and special formulas and depends upon the depth and von Karman roughness scale (z_o). The latter quantity is related to Manning's n value. In general, the effect of the wind stress is such that, for a given current, the effective resistance to the flow is reduced for a following wind and increased for an opposing wind, relative to the resistance which exists in the absence of the surface stress.

The special case of zero mean flow, in the presence of a surface stress, is treated as a special case of the general theory. The ratio between the bottom stress and surface stress (eq. (37) or (46)) depends upon the ratio of depth to the bottom roughness scale, and is found to be generally less than 1/10, which is at least in qualitative agreement with the available data pertinent to this problem (Van Dorn, (1953); Francis (1953)).

INTRODUCTION

For turbulent flow in an open channel, the shear stress τ_b (tangential force per unit area) exerted by the fluid on the channel bed (and sides) is asserted to be of quadratic form in respect to some gross velocity parameter; specifically

$$\tau_b = \rho \gamma_b^2 \; |v| \, v \tag{1}$$

where v is the average current for the cross-section of the channel concerned, ρ the density of the water and γ_b^2 is a non-dimensional proportionality factor* which depends upon the bottom roughness and channel dimensions (and shape). The stress is directed with the velocity (i.e., τ_b takes the sign of v as indicated by eq. (1)). The above assumption regarding the stress leads to the well established result that, under conditions of steady stream flow in a uniform channel, the mean current, hence the stream discharge through a given cross-section, is proportional to the square root of the surface slope along the axis of the channel (cf., Rouse, 1946, p. 217).

In tidal hydraulics eq. (1) is also used to evaluate the damping of seiches and long surges in channels (Proudman, 1955; Dronkers and Schonfeld, 1955; Ichiye, 1955). In both problems above (streaming flow and surging) it is understood that no surface stress occurs (or is negligible compared with bottom stress) and that as a consequence, the flow in the channel is very nearly uniform with respect to depth except very near the stream bed where a large velocity shear occurs, giving rise to the stress adjacent to the bed.

Turn next to the situation of a steady set-up of water in a bay or lake caused by a strong, sustained wind. In this case there is no net flow (v = 0), however a wind-induced current must occur near the surface requiring a return flow near the bottom to compensate for the surface flow (Hellstrom, 1941; Forssblad, 1947; Holmgren, et. al., 1944). A typical profile of such flow conditions is given in Figure 1. A detailed discussion of this graph is deferred until later. It is apparent that for flow of this type, the stress exerted by the fluid on the bottom is directed in the opposite sense to that of the wind.

*The term γ_b^2 is not to be confused with the wind resistance coefficient for the free water surface. Actually γ_b^2 is one-eighth of the Darcy-Weisbach coefficient commonly employed in conduit flow (Rouse, 1946, p. 201).

Furthermore, for a given channel the bottom stress under steady set-up conditions depends upon the wind stress only. Several theoretical studies dealing with this problem (Boussinesq, 1877; Hellstrom, 1941; Keulegan, 1951; Kivisild, 1954) have been made and a few direct measurements of the bottom stress under such conditions have been attempted. All of the theories indicate that for a given bottom roughness and depth, the bottom stress is proportional to the wind stress. The various theories differ widely in regard to the factor of proportionality. The measurements indicate that the ratio of the bottom stress to surface stress is of the order of 1/10 or less (Van Dorn, 1953). Most of the theoretical values for this ratio are higher, with the exception of the results given by Kivisild (1954, p. 77). In any event the bottom stress under the condition of zero net flow can have a significant influence on the slope or set-up of water in a channel, and acts so as to enhance the effect of the wind by impeding the subsurface return flow.

Obviously eq (1) fails completely for evaluating bottom stress in the problem of sustained wind-induced set-up of water. The equation could apply if the velocity v is reinterpreted as that which occurs at a small distance above the bottom. However the fact still remains that this velocity depends entirely upon the wind stress, for a given channel, and therefore so does the bottom stress.

Consider now the problem of evaluating the bottom stress in a flowing stream in the presence of a surface wind stress. If a strong wind acts in the direction of the stream, then a rapid decrease of velocity with depth must occur in the upper layers (Fig. 2A). This leads to the result that, <u>for a given discharge</u>, the velocity shear near the bottom is less than what it would be in the absence of the wind and hence the magnitude of the bottom stress is less than that predicted by eq (1). On the other hand if the wind acts against the flow then there will be an increase of velocity with depth in the upper layers, giving rise to a maximum velocity at some sub-surface level (Fig. 2B). The result in this case is that, <u>for a given discharge</u>, the velocity shear near the bottom must be greater than that which occurs in the absence of the wind stress and the bottom stress is accordingly greater in magnitude

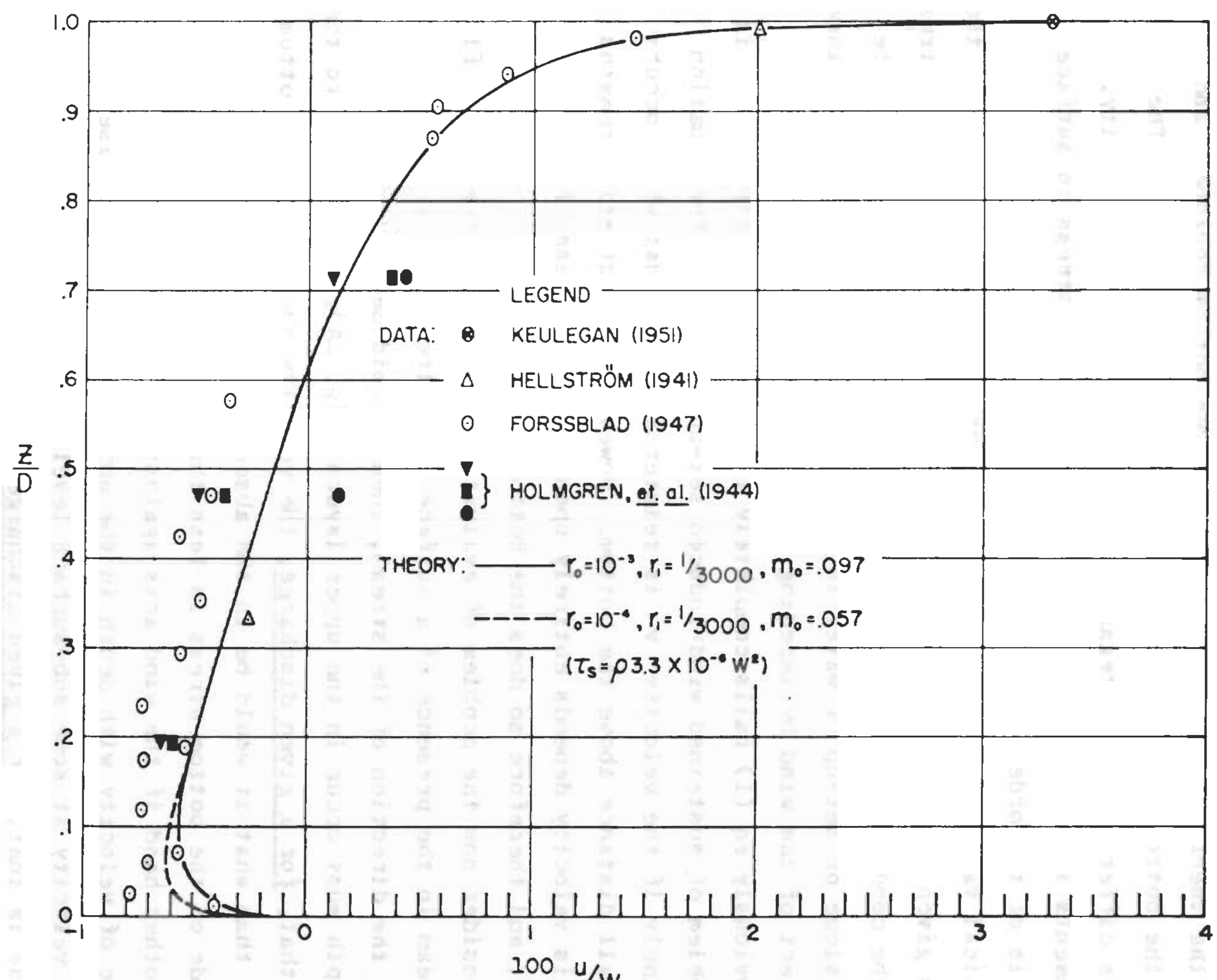

FIGURE 1

Relative velocity profile associated with equilibrium set-up conditions in a bounded channel

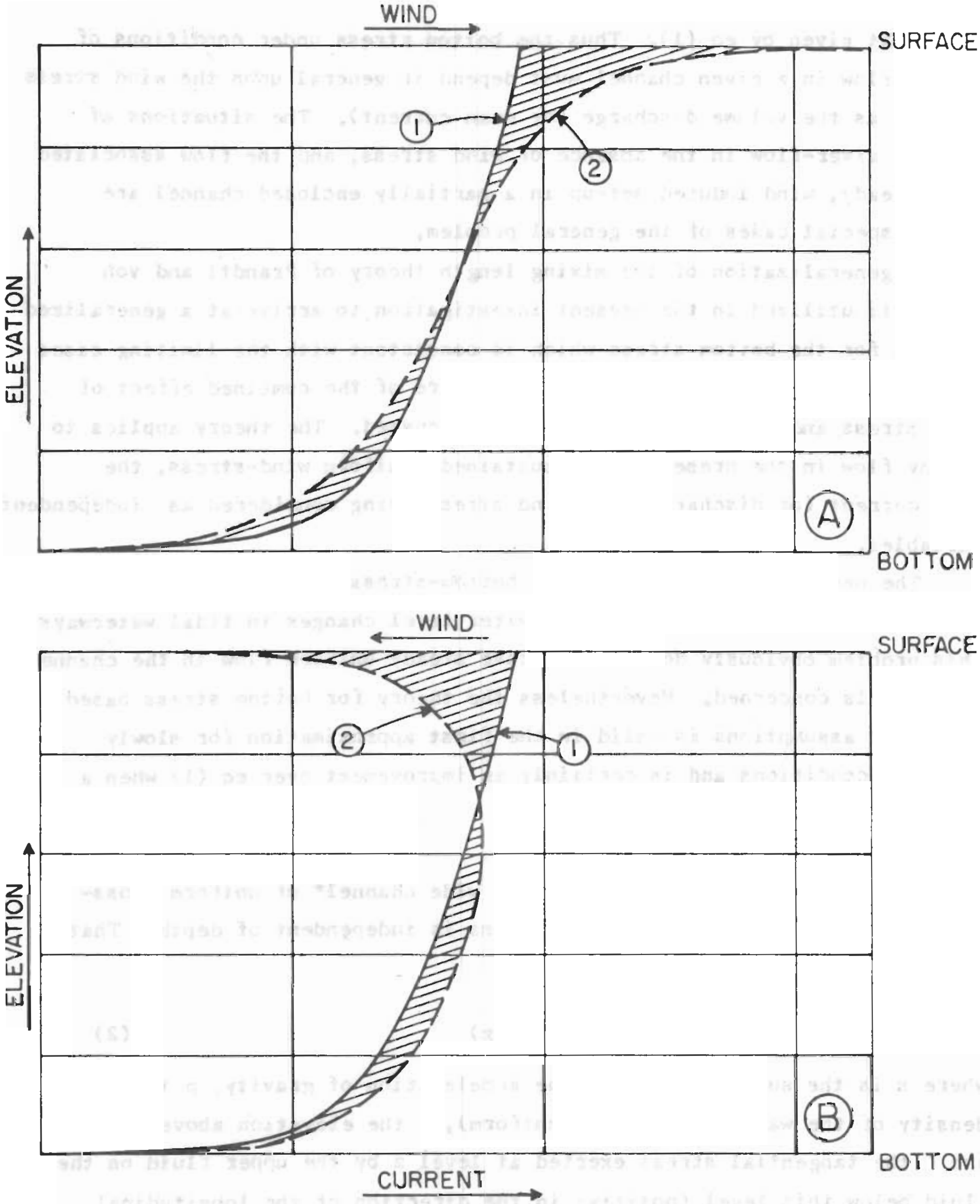

FIGURE 2

A. Schematic diagram indicating the effect of a following wind (curve (1) for no wind, curve (2) with a following wind); total volume transport the same for both curves

B. Schematic diagram indicating the effect of an opposing wind (curve (1) for no wind, curve (2) with an opposing wind); total volume transport the same for both curves than that given by eq (1). Thus the bottom stress under conditions of steady flow in a given channel must depend in general upon the wind stress as well as the volume discharge (or mean current). The situations of steady, river-flow in the absence of wind stress, and the flow associated with steady, wind induced set-up in a partially enclosed channel are simply special cases of the general problem.

A generalization of the mixing length theory of Prandtl and von Karman is utilized in the present investigation to arrive at a generalized formula for the bottom stress which is consistent with the limiting cases mentioned, and yields a quantitative measure of the combined effect of wind stress and mean current which was discussed. The theory applies to steady flow in the presence of a sustained, uniform wind-stress, the mean current (or discharge) and wind stress being considered as independent variables.

The necessity of a generalized bottom-stress formula arises in the problem of evaluating wind induced water level changes in tidal waterways. This problem obviously does not involve steady uniform flow in the channel or channels concerned. Nevertheless the theory for bottom stress based upon such assumptions is valid in the first approximation for slowly changing conditions and is certainly an improvement over eq (1) when a significant wind stress exists.

THEORY

Under steady flow conditions in a wide channel* of uniform cross-section, the vertical gradient of stress is independent of depth. That is

$$\frac{d\tau}{dz} = \rho g s \neq f(z) \qquad (2)$$

where s is the surface slope, g the acceleration of gravity, ρ the density of the water (considered uniform), z the elevation above bottom, and τ the tangential stress exerted at level z by the upper fluid on the fluid below this level (positive in the direction of the longitudinal coordinate x). Thus if τ_s is the stress at the free surface, τ_b the bottom stress, and D the depth of fluid, then it follows from (2) that

*Here we imply that the width is very large compared with the mean depth. The present theory does not take into account variations of stress across the channel, and the depth is considered as essentially constant across the channel. The influence of cross-section shape on flow characteristics in open channels is discussed by Keulegan (1938).

$$\tau = \tau_b + (\tau_s - \tau_b)\frac{z}{D} \quad (3)$$

where ρgs is replaced by the equivalent quantity $(\tau_s - \tau_b)/D$. The channel is considered wide enough that the side stress is of minor importance.

Following Prandtl and von Karman (cf., Bakhmeteff, 1936; Brunt, 1941, p. 244-46) the stress under conditions of turbulent flow is presumed to be related to the velocity shear as follows

$$\tau = L^2 \left|\frac{du}{dz}\right| \frac{du}{dz} \quad (4)$$

where u is the temporal mean velocity at level z in the x direction (along the channel axis). The mixing length L for flow in a semi-infinite fluid adjacent to a flat plate is considered as a linear function of distance from the plate:

$$L = k_o (z + z_o) \quad , \quad (5a)$$

where z is the distance from the boundary, k_o is a dimensionless constant, and z_o is a characteristic roughness length for the surface*. Experimental data indicate that the von Karman constant k_o is independent of the nature of the surface and has a value of approximately 0.40 (Rouse, 1946, p. 192). For flow in a channel or pipe wherein the boundary is not a simple plane and the cross-sectional area of fluid transverse to the flow is of limited extent, we cannot expect the simple relation (5a) to hold except very close to the boundary.

Montgomery (1943) has suggested a general formula for evaluating the distribution of L within a closed or open channel cross-section of any configuration. For flow in a semi-infinite fluid over a flat plate, the general formula leads to eq (5a), while for flow in a pipe Montgomery's hypothesis yields a non-linear dependence of L on radial distance from the pipe axis and leads to better agreement with data than the usual linear relation, provided that the stress is considered as a continuous

* The roughness parameter z_o is a small fraction (of the order of 1/10) of the mean diameter of the roughness elements. In the present paper we restrict the analysis to hydrodynamically rough surface conditions only.

functions of distance from the axis of the pipe* . For the case of flow in a wide channel with a free surface, the generalized mixing length hypothesis of Montgomery leads to the following quadratic form for the mixing length

$$L = \frac{k_o}{D} (z + z_o) (D + z_1 - z), \qquad (5)$$

where z_o is a characteristic roughness length for the channel bed and z_1 is a similar characteristic parameter for the free surface. The parameter z_1 is related to the wind induced waves on the surface. It will be considered throughout the present investigation that z_o and z_1 are <u>very small relative to D</u>. In this case eq (5) reduces essentially to eq (5a) very near the bottom, while near the free surface eq (5) reduces to a similar linear approximation:

$$L \doteq k_o \left[(D - z) + z_1\right] , \qquad (5b)$$

(D-z) being the distance below the free surface. These two asymptotic relations and the general relation (5) are illustrated in Fig. 3, where the values L_o and L_1 are very nearly equal to $k_o z_o$ and $k_o z_1$, respectively.

If the stress were uniform, then near the surface or bottom, where the mixing length is nearly linear, the velocity distribution according to eq (4) will obey the welll known log law (Rouse, 1946, p. 194), u being a linear function of log z. This still holds approximately when the stress varies; however, at intermediate depths the simple log law is transcended.

In the evaluation of the velocity distribution from eq (4), using the quadratic form of L given by eq (5) there are two general situations which must be considered separately. The first situation is that for which τ_b and τ_s are the same sign and the second where τ_b and τ_s are of opposite sign. It is convenient to introduce the following dimensionless variables to simplify the equations:

*Montgomery found that the best agreement was found with experimental data by taking k_o as 0.45 with his generalized theory. However, to be consistent with the more widely accepted value 0.40, we will adopt the latter value in the numerical calculations of this paper.

$$\left\{\begin{array}{ll}(a) & U = \dfrac{u}{\sqrt{\tau_s/\rho}} \\ (b) & m = \tau_b/\tau_s \\ (c) & \zeta = z/D \\ (d) & r_o = z_o/D \ll 1 \\ (e) & r_1 = z_1/D \ll 1\end{array}\right. \qquad (6)$$

In all cases (except where $\tau_s = 0$) it will be understood that the x axis is taken in the direction of τ_s, and the latter is therefore always positive. In the case of a stress opposing the mean current, the latter is taken negative.

Combining eqs (3), (4) and (5) and introducing the transformations (6) leads to the following differential equations for the current;

$$\frac{dU}{d\zeta} = \frac{\sqrt{m + (1 - m)\zeta}}{k_o\,(r_o + \zeta)\,(1 + r_1 - \zeta)}\ , \text{ if } m > 0 \qquad (7)$$

$$\left\{\begin{array}{lll}(a) & \dfrac{dU}{d\zeta} = \dfrac{\sqrt{|m| - (1 + |m|)\zeta}}{k_o\,(r_o + \zeta)\,(1 + r_1 - \zeta)}\ , & \text{if } m < 0,\ \zeta < \zeta_m \\ (b) & \dfrac{dU}{d\zeta} = \dfrac{\sqrt{(1 + m)\zeta - |m|}}{k_o\,(r_o + \zeta)\,(1 + r_1 - \zeta)}\ , & \text{if } m < 0,\ \zeta > \zeta_m\end{array}\right. \qquad (8)$$

where

$$\zeta_m = \frac{|m|}{1 + |m|}\ , \qquad (9)$$

which represents the relative elevation of the point of reversal of stress. The distributions of U and τ for the cases $m > 0$ and $m < 0$ are indicated schematically in Fig. 4.

The solution of eq (7) is complicated by the fact that the form of the solution depends upon the relative magnitude of m compared with r_o and r_1. The case of negative m (τ_b negative) is complicated by the fact that separate solutions are required above and below the point of stress reversal; however, these solutions hold for all negative values of m. The latter case will be treated first.

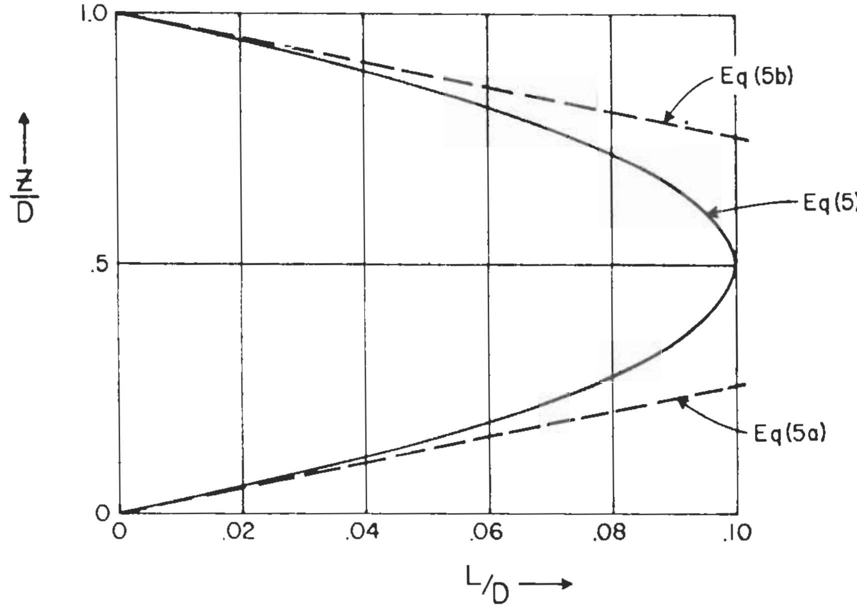

FIGURE 3

Dimensionless plot of mixing length versus depth (full curve) and asymptotic relations (dashed curves)

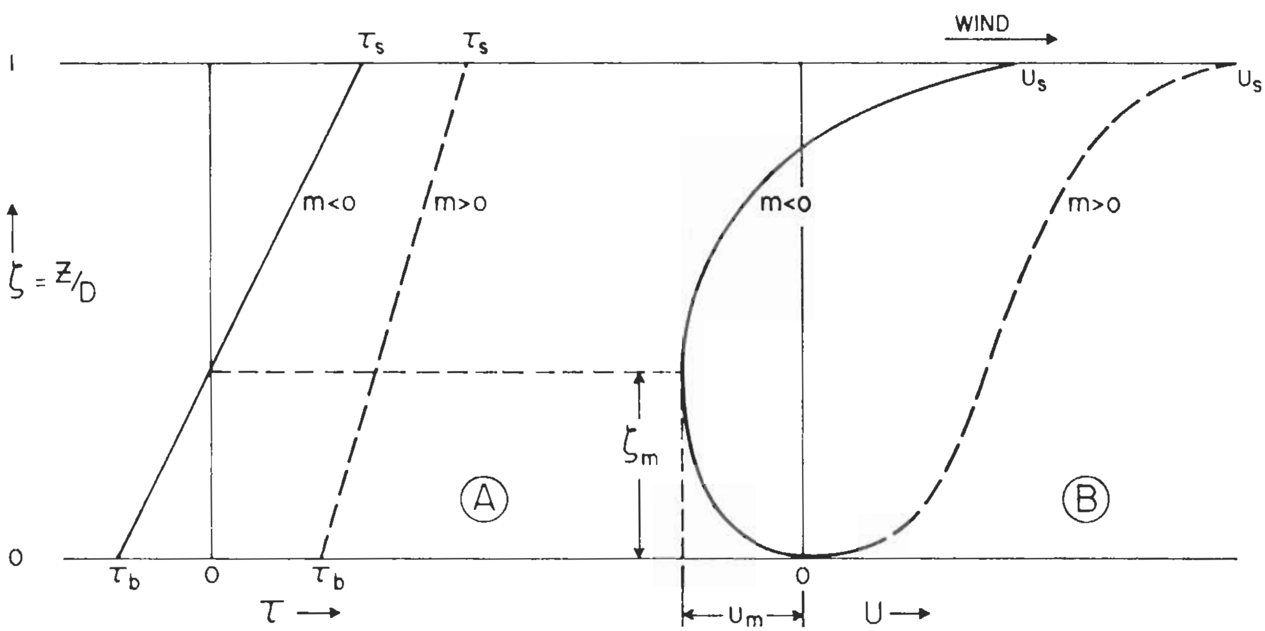

FIGURE 4

Shear stress distribution (A) and Associated current (B) (schematic) for the cases of negative m (full curves) and positive m (dashed curves). Note geometrical interpretation of ζ_m

VELOCITY DISTRIBUTION FOR NEGATIVE m

We require as a boundary condition that u and hence U be zero at the bottom. Furthermore the velocity must be continuous at the relative elevation ζ_m. Under these conditions it can be shown that the solution of eqs (8) are

$$U = -U_m - \frac{1}{k_o'}\left[B_o \ln \frac{B_o - y}{B_o + y} + 2B_1 \tan^{-1}\frac{y}{B_1}\right], \quad \text{for } \zeta < \zeta_m \tag{10a}$$

and

$$U = -U_m - \frac{1}{k_o'}\left[2B_o \tan^{-1}\frac{y}{B_o} + B_1 \ln \frac{B_1 - y}{B_1 + y}\right], \quad \text{for } \zeta > \zeta_m \tag{10b}$$

where

$$\left\{\begin{aligned} y &= \sqrt{|m + (1-m)\zeta|} \\ B_o &= \sqrt{|(1-m)\, r_o - m|} \\ B_1 &= \sqrt{|1 + (1-m)\, r_1|} \\ k_o' &= k_o(1 + r_o + r_1)\,. \end{aligned}\right. \tag{11}$$

Furthermore

$$U_m = \frac{1}{k_o'}\left[B_o \ln \frac{B_o + \sqrt{|m|}}{B_o - \sqrt{|m|}} - 2B_1 \tan^{-1}\sqrt{\frac{|m|}{B}}\right], \tag{12}$$

which represents the relative velocity at the point of stress reversal (ζ_m) and is therefore the maximum value of negative velocity (Fig. 4B), since at this point the stress and hence the velocity shear are zero (Fig. 4A). Inasmuch as r_o and r_1 are to be regarded as very small compared with unity, the factor k_o' can be replaced by k_o without serious error. Furthermore since $|m|$ in most applications is much larger than r_o or r_1, the above relations can be put in a more convenient form. For this situation, the following approximations are applicable

$$\left\{\begin{aligned} B_o &\doteq \sqrt{|m|} + \frac{(1 + |m|)r_o}{2\sqrt{|m|}}\,, \\ B_1 &\doteq 1 + \frac{1}{2}(1 + |m|)r_1\,, \end{aligned}\right. \quad \text{for } |m| \gg r_o,\ r_1 \tag{13}$$

and neglecting terms of minor importance, eq. (12) takes the approximate form

$$U_m \doteq \frac{1}{k_o}\left[\sqrt{|m|}\ \ln \frac{4|m|}{(1+|m|)r_o} - 2\tan^{-1}\sqrt{|m|}\right] \tag{12a}$$

$$\text{for } r_o, r_1 \ll 1, \; m < 0$$

The relative surface current as deduced from (10b) and the above approximations is given by

$$U_s = \frac{1}{k_o}\left\{\ln\frac{4}{(1+|m|\,r_1} + 2\tan^{-1}\sqrt{|m|} - \sqrt{|m|}\left[\ln\frac{4|m|}{(1+|m|)r_o} + 2\tan^{-1}\frac{1}{\sqrt{|m|}}\right]\right\} \quad \text{for } r_o, r_1 \ll, \; m < 0 \tag{14}$$

where $U_s\sqrt{\tau_s/\rho} = u_s$ is the surface current. Notice that, to the approximation given, the value of U_m is independent of r_1 (the free surface roughness ratio); on the other hand U_s depends rather critically upon r_1 as should be expected*. Some example velocity distributions evaluated from eqs.(10a,b) and the approximations (13) and 12a) are shown in Fig. 5.

MEAN CURRENT FOR NEGATIVE m

The mean current v is defined by

$$v \equiv \frac{1}{D}\int_0^D u\,dz \tag{15}$$

We will denote by V the relative mean current which can be determined from the relation

$$V \equiv \frac{v}{\sqrt{\tau_s/\rho}} = \int_0^1 U\,d\zeta \tag{16}$$

In the case of negative m we must perform the integration in two parts as follows:

$$V = \int_0^{\zeta_m} U_a\,d\zeta + \int_{\zeta_m}^1 U_b\,d\zeta \tag{17}$$

where U_a and U_b are the functions given by eqs. (10a) and (10b) respectively (for the method of integration see Appendix A). The result for negative m is

$$V \doteq \frac{2}{k_o}\left\{(1+\sqrt{|m|}) - B_o\left[\tan^{-1}\frac{1}{B_o} + \frac{1}{2}\ln\frac{B_o+\sqrt{|m|}}{B_o-\sqrt{|m|}}\right]\right\} \tag{18}$$

*Note that U_s approaches infinity as r_1 approaches zero, but the velocity shear also approaches infinity at the surface in such a way that very little effect is felt at subsurface depths due to a change in r_1.

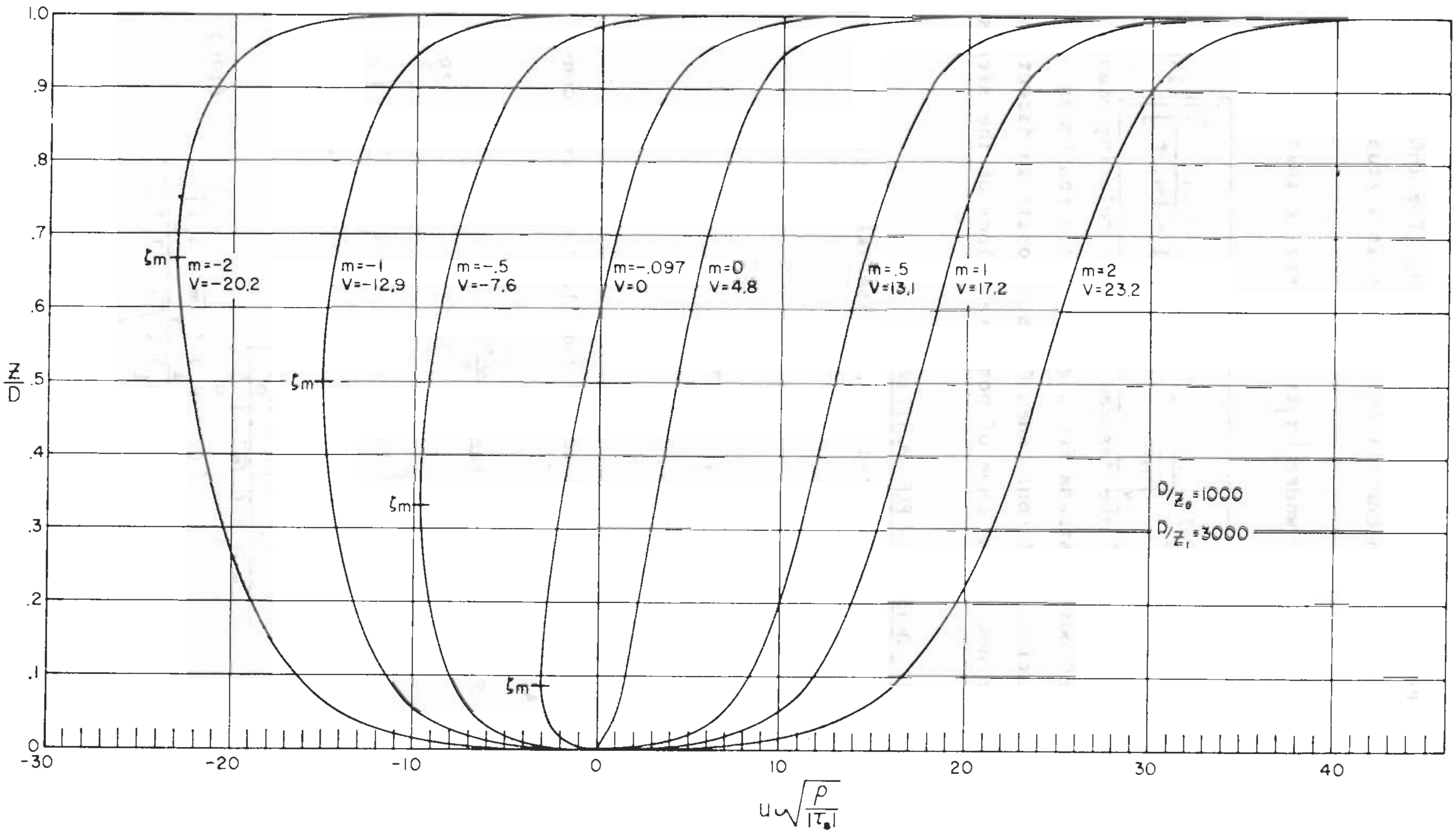

FIGURE 5

Graphs of the computed relative current $U = u\sqrt{\rho/|\tau_s|}$ versus relative elevation for eight different values of m (associated values of the dimensionless mean current V are indicated along with m); computations are based upon eqs (10) through (12) and (18) for m < 0, and upon eqs (19a, b, c, d) and (21) for m > 0. All computations are based upon $r_o = 10^{-3}$ and $r_1 = 1/3000$.

where terms of very minor importance have been dropped. The influence of the magnitude of r_1 on the mean current for example is virtually nil (Appendix A).

If we consider again the case where $|m|$ is much greater than r_o then eq (18) approximates to

$$\boxed{V \doteq \frac{2}{k_o}\left\{(1+\sqrt{|m|}) - \sqrt{|m|}\left[\tan^{-1}\frac{1}{\sqrt{|m|}} + \frac{1}{2}\ln\frac{4|m|}{(1+|m|)r_o}\right]\right\}} \quad (18a)$$

Eq (18) or (18a) represents one of the desired equations relating mean current, wind stress, and bottom stress for a given bottom roughness anddepth; the cited equations apply only when τ_b is opposite in direction to τ_s $(m < 0)$. We turn now to the case of positive values of the stress ratio m.

VELOCITY DISTRIBUTION FOR POSITIVE m

Four separate solutions are required for positive values of m accordingly as:

(A) $0 \leqslant m \leqslant r_o/(1 + r_o)$

(B) $r_o/(1+ r_o) \leqslant m \leqslant (1 + r_1)/r_1$, $m \neq 1$

(C) $m = 1$

(D) $m \geqslant (1 + r_1)/r_1$

It can be verified that the solutionsof eq (7) for these different conditions are, for case A:

$$U = \frac{1}{k_o'}\left\{2B_o\left[\tan^{-1}\frac{y}{B_o} - \tan^{-1}\frac{\sqrt{m}}{B_o}\right] - B_1\left[\ln\frac{B_1 - y}{B_2 + y} - \ln\frac{B_1 - \sqrt{m}}{B_1 + \sqrt{m}}\right]\right\}; \quad (19a)$$

for case B:

$$U = \frac{1}{k_o'}\left\{B_o\ln\left[\frac{(y - B_o)(\sqrt{m} + B_o)}{(y + B_o)(\sqrt{m} - B_o)}\right] - B_1\ln\left[\frac{(y - B_1)(\sqrt{m} + B_1)}{(y + B_1)(\sqrt{m} - B_1)}\right]\right\}; \quad (19b)$$

for the singular case $C(\tau_b = \tau_s)$:

$$U = \frac{1}{k_o'}\left[\ln\frac{r_o + \zeta}{r_o} - \ln\frac{1 + r_1 - \zeta}{1 + r_1}\right]; \qquad (19c)$$

and finally for case D

$$U = \frac{1}{k_o'}\left\{B_o \ln\left[\frac{(B_o - y)(B_o + \sqrt{m})}{(B_o + y)(B_o - \sqrt{m})}\right]\right.$$
$$\left. + 2B_1\left[\tan^{-1}\frac{y}{B_1} - \tan^{-1}\frac{\sqrt{m}}{B_o}\right]\right\} \qquad (19d)$$

where y, B_o, B_1, k_o', are defined by eq (11). In all cases the constant of integration is taken such that U (hence the current u) reduces to zero at the bottom ($\zeta = 0$).

It will be noted that in the special case of $m = 0$ eq (19a) and (10b) each reduce to the form

$$U = \frac{1}{k_o'}\left\{\sqrt{1 + r_1}\ \ln\frac{\sqrt{1 + r_1} + \sqrt{\zeta}}{\sqrt{1 + r_1} - \sqrt{\zeta}} - 2\sqrt{r_o}\ \tan^{-1}\sqrt{\frac{\zeta}{r_o}}\right\} \qquad (20)$$

thus assuring a continuous transition from the case of negative m to that of positive m*. Example velocity distribution for the case of positive m, eqs (19), are compared with those for negative m in Fig. 5.

MEAN CURRENT FOR POSITIVE m

Using eqs (19a) to (19d) in eq (16) yields the following equations for the dimensionless mean current, V, under the condition that r_o and r_1 are very small (see Appendix A for details): for $0 \leq m \leq r_o/1 + r_o$

$$V = \frac{2}{k_o}\left\{(1 - \sqrt{m}) - B_o\left[\tan^{-1}\frac{1}{B_o} - \tan^{-1}\frac{\sqrt{m}}{B_o}\right]\right\}; \qquad (21)$$

for $m \geq r_o/1 + r_o$, $m \neq 1$

$$V = \frac{2}{k_o}\left\{(1 - \sqrt{m}) + 1/2\, B_o \ln\left[\frac{(\sqrt{m} + B_o)(1 + B_o)}{(\sqrt{m} - B_o)(1 - B_o)}\right]\right\} \qquad (22)$$

and for $m = 1$

$$V = V_1 = \frac{1}{k_o}\ln\frac{4}{r_o} \qquad (23a)$$

*Some question may arise here as to the applicability of the hydrodynamically rough surface theory in the case of very small τ_b (hence small m). When τ_b is less than a certain value it may be expected that a laminar sublayer develops near the boundary. This possibility is not explored in the present paper, and probably should be investigated.

For m exceeding $(1 + r_1)/r_1$ eq(22) is still an adequate approximation (see Appendix A). Essentially the above approximations are very good as long as r_o and r_1 are less than about 10^{-2}.

When $m >> r_o$ then eq (22) approximates to the more convenient form

$$\boxed{V = \frac{2}{k_o}\left\{(1 - \sqrt{m}) + \sqrt{m}\ \ln \frac{\sqrt{m}}{(1 + \sqrt{m})} + 1/2\sqrt{m}\ \ln \frac{4}{r_o}\right\}} \tag{22a}$$

The range of V for m lying between 0 and r_o is quite small. For $m = 0$, eq (18a) and (21) each reduce to the relation

$$V = V_o \equiv \frac{2}{k_o}\left[1 - \sqrt{r_o}\ \tan^{-1}\frac{1}{\sqrt{r_o}}\right] \tag{23}$$

while for $m = r_o/(1 + r_o)$, eq (21) and (22) each reduce to

$$V = \frac{2}{k_o}(1 - \sqrt{r_o}), \tag{24}$$

again assuring a continuous relation between V and m. Since we will be concerned with values of $r_o < 10^{-2}$ ($z_o < D/100$) it follows that the range in V, corresponding to $0 < m < r_o$, is less than about 6 percent of V_o. For this reason eqs (18a) and (22a) relating v, τ_b, and τ_s are of primary concern since they are applicable to almost the entire range of the variables concerned, with the exception of very small m (of the order of r_o). Before discussing this relationship in detail we will examine a few special cases of immediate interest.

STEADY FLOW IN THE ABSENCE OF SURFACE STRESS

In the case of $\tau_s = 0$, eq (10a) and eq (19b) reduce* to the common form

$$u = \pm \frac{1}{k_o}\sqrt{\frac{\tau_b}{\rho}}\left\{\sqrt{1 + r_o}\ \ln \frac{(\sqrt{1 + r_o} - \sqrt{1 - \zeta})(\sqrt{1 + r_o} + 1)}{(\sqrt{1 + r_o} + \sqrt{1 - \zeta})(\sqrt{1 + r_o} - 1)} + 2\sqrt{r_1}\left[\tan^{-1}\frac{\sqrt{1 - \zeta}}{\sqrt{r_1}} - \tan^{-1}\frac{1}{\sqrt{r_1}}\right]\right\} \tag{25}$$

which in the case of very small r_o and r_1 approximates to

$$u = \pm \frac{1}{k_o}\frac{\tau_b}{\rho}\ \ln\left[\frac{(1 - \sqrt{1 - \zeta} + 1/2 r_o)}{(1 + \sqrt{1 - \zeta})}\ \frac{4}{r_o}\right] \tag{26}$$

*In this case it is necessary to multiply eqs (10a) and (19b) by $\sqrt{\tau_s/\rho}$ before setting τ_s equal to zero.

where the signs in eqs (25) and (26) are taken to agree with that of τ_b. Very near the bottom ($\zeta \ll 1$) eq (26) approaches the simple form

$$u = \pm \frac{1}{k_o} \sqrt{\frac{\tau_b}{\rho}} \ln \frac{z + z_o}{z_o} \tag{27}$$

which will be recognized as the celebrated Prandtl-von Karman log law for turbulent flow over a flat plate, when the stress is considered uniform (Rouse, 1946, p. 195). This is of course only an approximation since τ decreases to zero at the free surface in the absence of wind. The more general relation (25) or (26) must be used at large distances above bottom. The velocity distribution based upon (25) for $r_o = 10^{-3}$ and $r_1 = 1/3000$ is shown in Fig. 6 (curve 1). The approximate relation (27) is shown for comparison (curve 2). Also shown are the distribution of current for the special cases $\tau_s = \pm \tau_b$, for the same values of r_o and r_1. The full curve for $\tau_s = 0$ has an inflection very close to the free surface, and above this inflection the slope reduces to zero in order to satisfy the condition of zero stress at the surface. If r_1 is taken as zero then the inflection point moves up to the surface. In this case the slope at the free surface does not vanish but the stress is zero since the mixing length is zero for vanishing r_1.

The relation of more immediate concern is that connecting v and τ_b for the special case of $\tau_s = 0$. Equations (18a) and (22a) reduce to the form

$$v = \pm \frac{1}{k_o} \sqrt{\frac{\tau_b}{\rho}} \left(\ln \frac{4}{r_o} - 2\right) \tag{28}$$

where again the sign is taken to agree with that of τ_b. It follows immediately from (28) that

$$\tau_b = \rho \gamma_b^2 |v| v \text{ , for } \tau_s = 0 \tag{29}$$

where

$$\boxed{\gamma_b = k_o \left(\ln \frac{4D}{z_o} - 2\right)^{-1},} \tag{30}$$

Thus eq (1) is simply a limiting case of the more general relations (18a) and (22a) when τ_s is very small compared with τ_b. The dimensionless

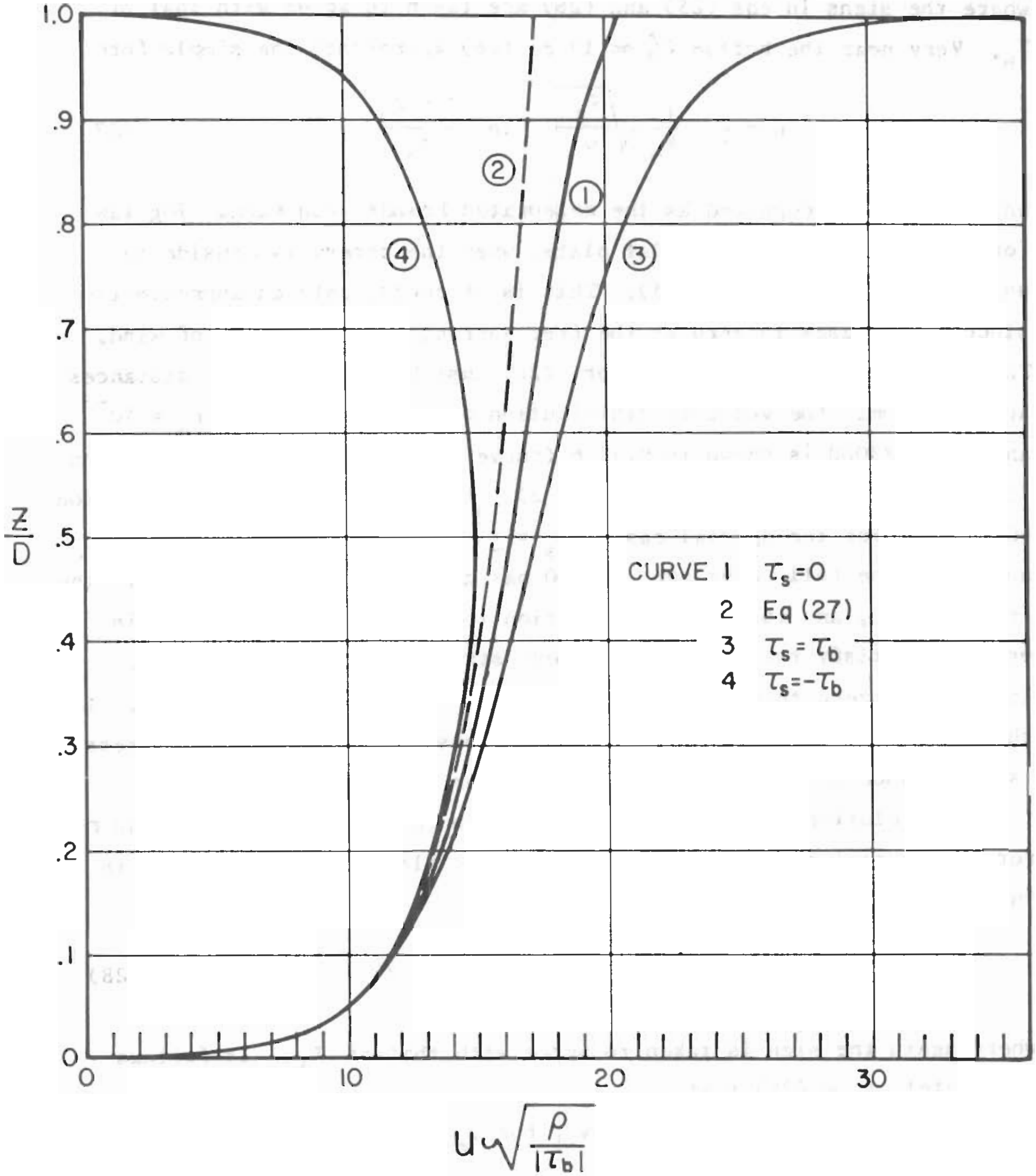

FIGURE 6

Comparison of computed relative currents $u\sqrt{\rho/|\tau_b|}$ versus relative elevation for the cases $\tau_s = \pm\tau_b$ and $\tau_s = 0$ (i.e., $m = \pm 1$ and 0). Computations are based upon $r_o = 10^{-3}$ and $r_1 = 1/3000$

parameter γ_b^2 will hereafter be referred to as the bed resistance coefficient and is a characteristic parameter of the channel. Note that it varies only with the relative roughness of the channel bed (z_o/D).

In computations of river discharge, Manning's empirical formula is frequently used. It can be shown that his formula leads to the following representation for γ_b (Rouse, 1946, p. 217-18)*.

$$\gamma_b = 3.82\ n/D^{1/6} \tag{31}$$

where Manning's n has the units of $(\text{feet})^{1/6}$. Comparing eqs (30) and (31) we see that z_o and Manning's n, representing different parameters for characterizing the bed roughness, can be related by equating the two expressions for γ_b. This leads to the relation

$$\frac{n}{z_o^{1/6}} = \frac{0.105\ (D/z_o)^{1/6}}{(\ln \frac{4D}{z_o} - 2)} \tag{32}$$

where von Karman's constant k_o is taken as 0.40. A graph of $n/z_o^{1/6}$ versus D/z_o is shown in Figure 7 (curve 1). It will be noticed that the ratio $n/z_o^{1/6}$ lies in the range 0.053 to 0.066 for D/z_o varying from 100 to 100,000. Thus for all practical purposes the ratio is nearly independent of relative depth. If we adopt a mean value of 0.056, then n and $z_o^{1/6}$ are related approximately as shown in Fig. 8. Furthermore using the approximate relation

$$n \doteq 0.056\ z_o^{1/6} \tag{32a}$$

in eq (31) gives

$$\gamma_b \doteq 0.214\ (z_o/D)^{1/6} \tag{33}$$

This relation is compared graphically with eq (30) in Fig. 7 (curves 3 and 2 respectively). Any one of the parameters n, z_o, or γ_b can serve as a fundamental frictional parameter which together with the depth D characterize the particular channel concerned.

*Here the depth D is taken as equivalent to the hydraulic radius; this is justifiable if the channel width is of the order of 100 times the depth.

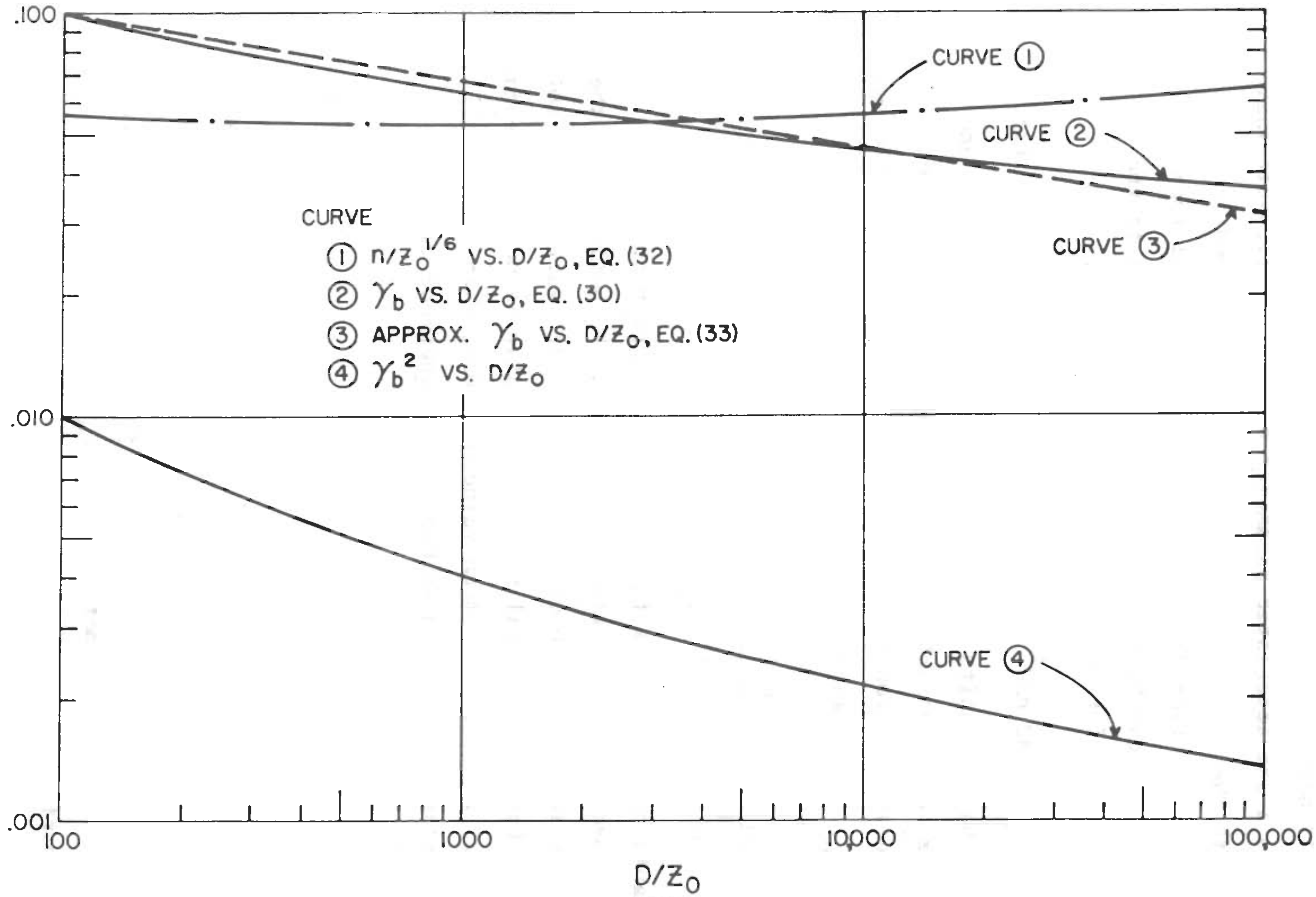

FIGURE 7

Curve (1): relationship between Manning's n, z_o and D.
Curve (2): the dimensionless factor γ_b versus D/z_o as deduced from the present theory.
Curve (3): the approximate 1/6 power law relation for γ_b using the relation of Fig. 8 and Manning's equation.
Curve (4): the bottom resistance coefficient γ_b^2 versus D/z_o (as obtained from eq. 30 or curve (2)).

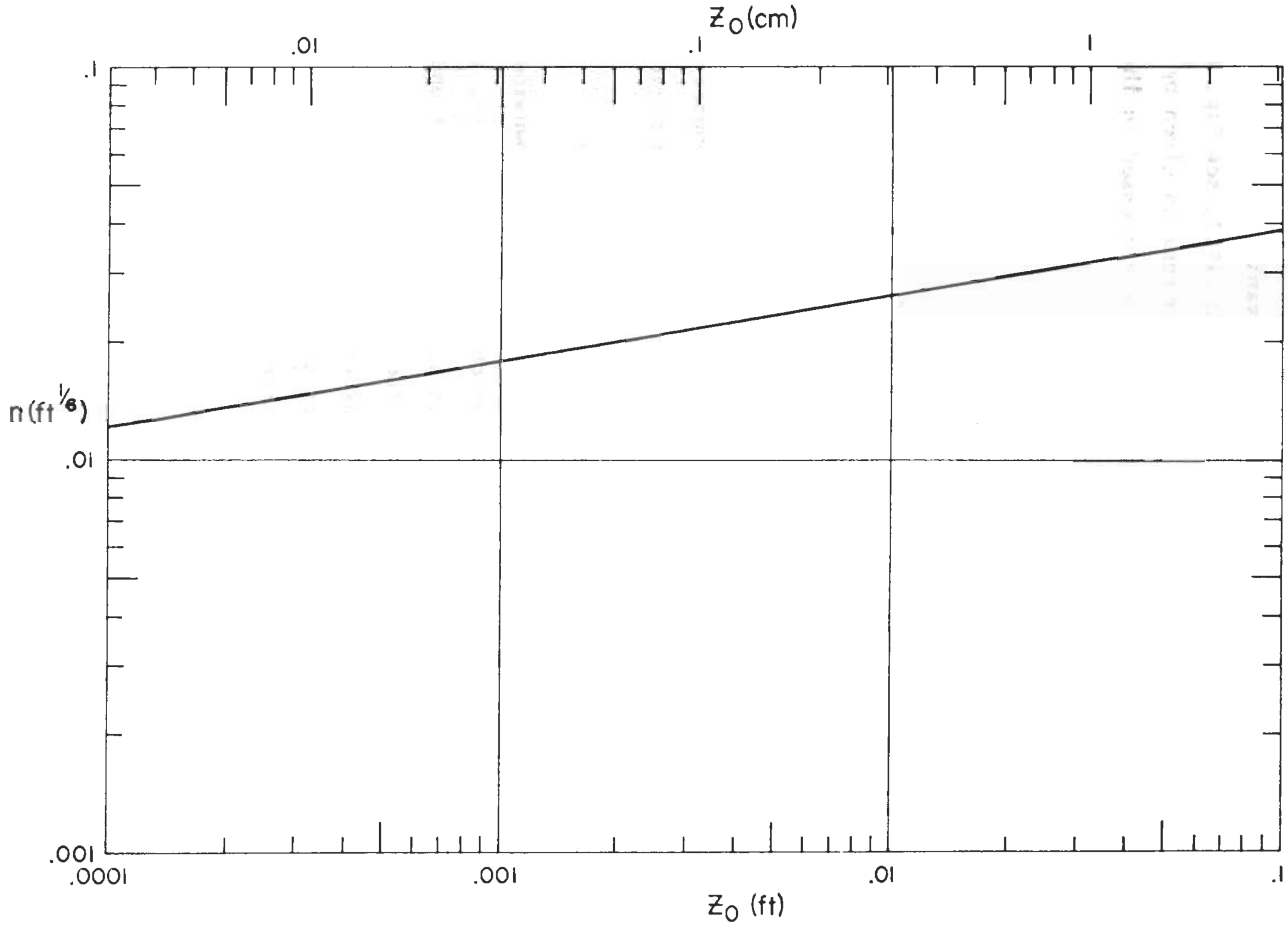

FIGURE 8

Approximate relation between Manning's n and the von Karman bottom roughness parameter z_o

PURE WIND-DRIVEN CURRENT IN AN UNBOUNDED CHANNEL

In the special case where $\tau_b = \tau_s$ (uniform stress from top to bottom) the surface slope is zero. That is, there is no gravitational force inducing the motion of the water; hence the current is purely wind driven and steady, since the gradient of the stress vanishes (curve 3). In this case the velocity distribution is given by eq (19c), see Fig. 6 (curve 3) for illustration of this case. The mean current is given by the simple relation (23a). The latter relation can be expressed in the form

$$V_1 = \gamma_b^{-1} + \frac{2}{k_o} \qquad (34)$$

in view of eq (30). Hence we have

$$\gamma_b = \frac{1}{\frac{2}{k_o} + V_1} = \frac{1}{5 + \frac{V}{\sqrt{\tau_s/\rho}}} \quad \text{, for } \tau_b = \tau_s \qquad (35)$$

This relation could be of value in estimating the resistance coefficient for an ungated canal during times of sustained strong wind along its axis, provided that no head differential were developed at the opposite ends of the canal. This would require slack water conditions in regard to tides or surges, such that the current is truly wind driven.

WIND SET-UP IN A BOUNDED CHANNEL OR PARTIALLY ENCLOSED BASIN

For steady state wind set-up in a channel bounded at the downwind end, the discharge through each section of the channel must be zero, i.e., the mean current vanishes (hence V = 0). This situation can exist only if the shear stress exerted on the bottom by the fluid is opposite to that at the surface, the flow in the lower layers of the channel being opposite to that at the surface. With respect to a vertical column of fluid of unit horizontal cross-section, the stresses τ_b and τ_s add in their effect and just balance the net force due to the surface slope (Fig. 9).

For the condition of V = 0 we will let

$$\left| \frac{\tau_b}{\tau_s} \right| = m_o \qquad (36)$$

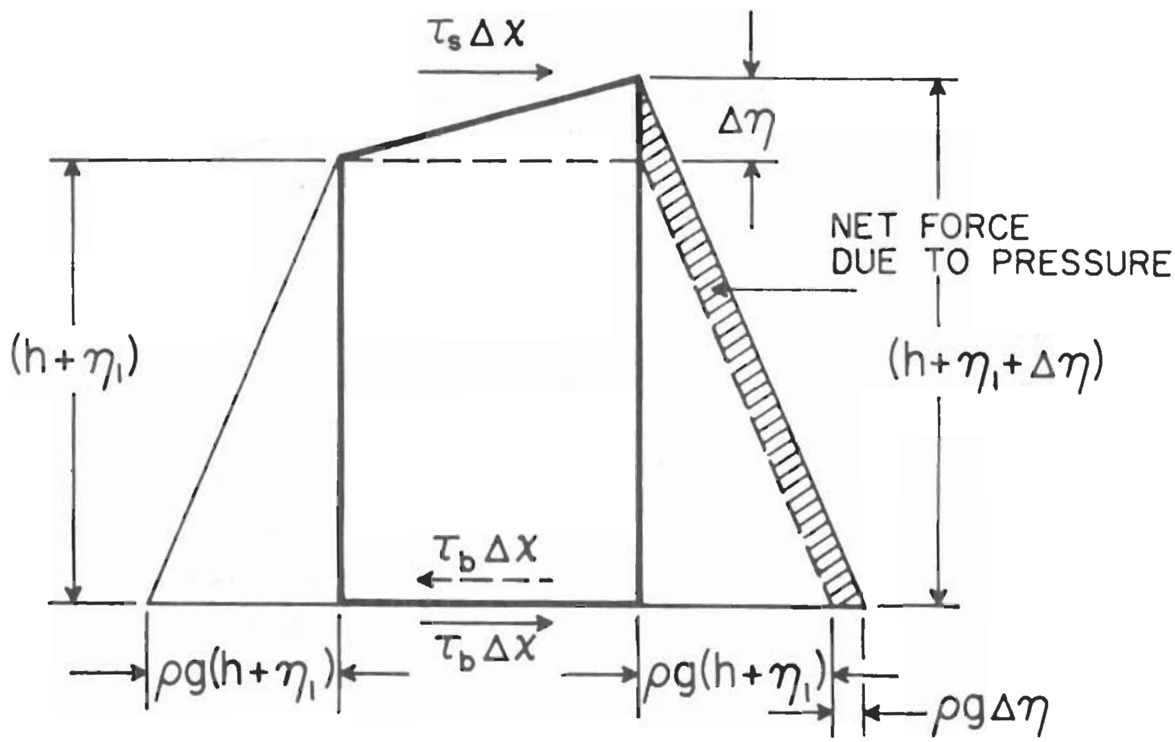

FIGURE 9

Schematic of the balance of forces on a vertical column of water of unit width, axial length Δx, and depth $h + \eta$. The net pressure force is $\rho g(h + \eta)\Delta\eta$ which under equilibrium conditions must balance the total external shear force which is $(|\tau_s| + |\tau_b|)\Delta x$ for this case.

For $r < 10^{-2}$, eq. (18a) can be used to evaluate m as an implicit function of the bottom roughness ratio $r_o = z_o/D$. Thus

$$\ln\left(\frac{D}{z_o}\right) = 2\left[1 + \frac{1}{\sqrt{m_o}} - \tan^{-1}\frac{1}{\sqrt{m_o}} + \frac{1}{2}\ln\frac{1+m_o}{4m_o}\right] \quad (37)$$

A plot of m_o versus D/z_o is shown in Fig. 10 (curve 1). This curve is compared with the theoretical relations obtained by Kivisild (1954) curves (2) and (3). A discussion of the latter relations is given in Appendix B. Hellstrom (1941) arrived at much higher values of m_o; 0.30 for a channel depth of 1 meter and 0.15 for a depth of 100 meters. If we consider that z_1 is of the order of 0.2 cm for a rippled sand or gravel bed then the above values of m_o correspond to $D/z_o = 500$ and and 50,000 respectively. This would indicate that the m_o values of Hellstrom are roughly threefold greater than those of the present theory.

Direct measurements of bottom stress by Van Dorn (1953) in a model yacht pond of 6 feet mean depth indicated a value of m_o of less than 0.1 for D/z_o of the order of 10^3 to 10^4. Laboratory tests conducted by Francis (1953) indicate an m_o value of only 0.014 for a tank of 44-cm depth with a wood floor. If we take an equivalent sand roughness diameter ($z_o/30$) of 0.053 cm (Keulegan, 1938) then the above value of m_o corresponds to D/z_o equal to about 25,000.

The velocity distribution for the case of $V = 0$ in the present theory can be obtained from eqs (10a, b) together with eq (12a). It will be noted that r_1 must be known as well as r_o in order to evaluate the velocity distribution. Actually, the value of r_1 is important only in the determination of the surface current u_s. Below the surface, the velocity distribution is quite insensitive to the value of r_1, (provided that r_1 is less than about 10^{-2}).

We can obtain an estimate of r_1 in relation to r_o for the condition of $V = 0$, from laboratory tests carried out by Keulegan (1951). Keulegan found that for sufficiently large depths (hence large D/z_o) the measured surface current approaches a limiting value of about 3.3 percent of the wind speed. If we take the surface stress as

$$\tau_s \doteq 3.3 \times 10^{-6}\, \rho W^2 \quad (38)$$

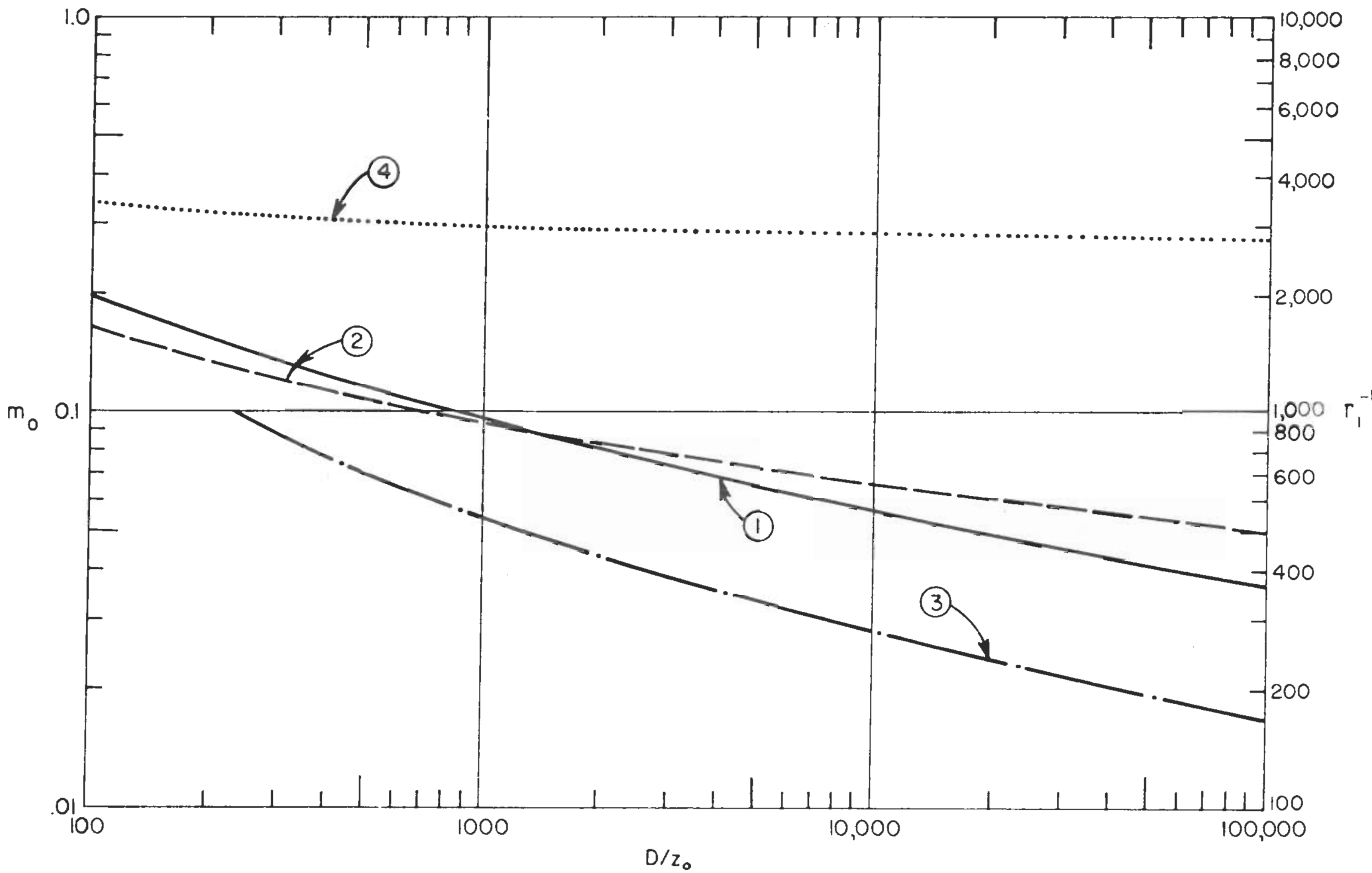

FIGURE 10

Curve (1): graph of m_o versus D/z_o computed from eq (37) (present theory).
Curve (2): graph of m_o versus D/z_o using eq. 4.4.11 of Kivisild's paper (1954), or eq. (B-1) of Appendix B.
Curve (3): graph of m_o versus D/z_o using eq 4.5.9 of Kivisild's paper (1954), or eq (B-2) of Appendix B.
Curve (4): graph of r_1^{-1} versus D/z_o evaluated from eqs (14), (37) and the approximate relation (39) deduced from Keulegan's experiments (1951).

where W is the wind speed along the channel axis (Beach Erosion Board, Technical Memorandum No. 27, 1952, p. 9) then

$$U_s = \frac{u_s}{\sqrt{\tau_s/\rho}} \doteq 18.2 \,, \qquad (39)$$

for the case of zero net flow (V = 0). Using eq (37) and (39) in eq (14) yields r_1 as a function of D/z_o. A plot of this relation is shown in Fig 10 (curve 4). It will be noted that r_1 is nearly independent of D/z_o and for all practical purposes we can use a mean value of r_1 of about 1/3000. Thus the surface roughness parameter z_1 is approximately 1/3000 of the depth, for steady set-up conditions.

The velocity distribution for the case of V = 0, taking $r_o = 10^{-3}$ and 10^{-4} and $r_1 = 1/3000$ is illustrated in Fig. 1 (full and dashed curves respectively). Relation (38) has been used to convert U to u/W. This allows direct comparison with empirical values of u/W (also shown in Fig. 1).

RELATION BETWEEN m, V, and r_o

Eqs (18a) and (22a) give m implicitly in terms of V for a given value of r_o provided that $|m| >> r_o$. These equations can be written in the form

$$V = -\left[\gamma_b^{-1} \sqrt{|m|} - f_1(m)\right] \,, \quad m < 0 \qquad (40a)$$

$$V = \left[\gamma_b^{-1} \sqrt{m} - f_2(m)\right] \,, \quad m > 0 \qquad (40b)$$

where

$$f_1(m) = \frac{2}{k_o} \left\{ \sqrt{|m|} \left[\frac{1}{2} \ln \frac{1 + |m|}{|m|} - \tan^{-1} \frac{1}{\sqrt{|m|}} \right] + 1 \right\} \qquad (41a)$$

$$f_2(m) = \frac{2}{k_o} \left\{ \sqrt{|m|} \ln \frac{1 + \sqrt{m}}{\sqrt{m}} - 1 \right\} \qquad (41b)$$

For m = 0 relation (23) yields the appropriate value of V.

Since both $f_1(m)$ and $f_2(m)$ approach zero as $|m|$ approaches infinity it follows that the quantity V' defined by

$$\begin{cases} V' = -\gamma_b^{-1} \sqrt{|m|} \,, & m < 0 \\ V' = \gamma_b^{-1} \sqrt{|m|} \,, & m > 0 \end{cases} \qquad (42)$$

is an asymptotic form of the general relation for V. It is therefore convenient to plot V versus $m/\sqrt{|m|}$ since the asymptotes will be straight lines running through the origin, the slopes of which are determined by r_o alone. The general relation of V versus $m/\sqrt{|m|}$ for the three different values of r_o are shown in Fig. 11 (full curves); the asymptotes as determined from eq (42) are also shown (dash-dot lines). The dotted curves and circled points refer to an approximate formula discussed in the next section.

EXPLICIT RELATION FOR BOTTOM STRESS

Equations (40a, b) yield V explicity in terms of m. More frequently it is necessary to know m explicitly in terms of V. Fig. 11 is sufficient for this purpose from the graphical standpoint. However, it is frequently necessary to express τ_b, hence m, explicitly as a function of v and τ_s in the form of an equation. This is particularly true in respect to computations of τ_b by high speed digital computers, wherein the use of a formula is usually more efficient than storage of a table of numerical values.

The following formula* is an approximation to the relation (40a,b) which yields values of m to an accuracy consistent with the approximations introduced in deriving eqs (40a,b):

$$m = \pm \gamma_b^2 \left[V - G(\alpha)\right]^2 \tag{43}$$

where the sign is taken consistent with V - G. The function $G(\alpha)$ is given by

$$\begin{cases} \text{(a)} \quad G(\alpha) = \dfrac{5}{1 + 2|\alpha|} + \dfrac{1.90\sqrt{|\alpha|}}{0.48 + \alpha^2}, & \alpha < 0 \\[2ex] \text{(b)} \quad G(\alpha) = \dfrac{5}{1 + 2\alpha} - \dfrac{0.15\sqrt{\alpha}}{0.043 + \alpha^2}, & \alpha > 0 \end{cases} \tag{44}$$

where

$$\alpha = \gamma_b \,(V - V_o) \tag{45}$$

and V_o is given by eq (23), which for very small r_o can be taken equal to 5 for all practical purposes.

---

* For methods of derivation see Appendix C.

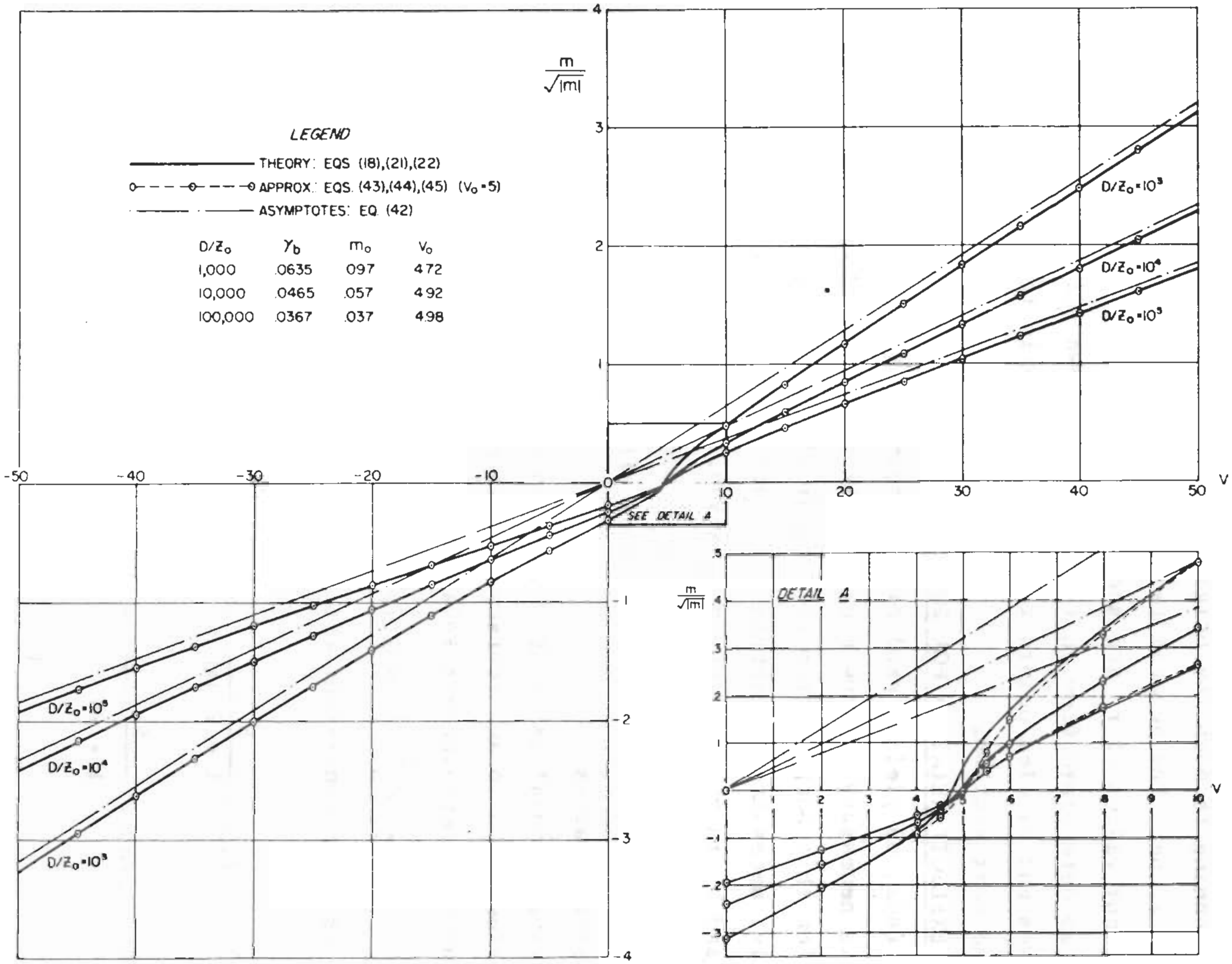

FIGURE 11

Graphs of the dimensionless stress parameter m versus the dimensionless mean current V for three selected values of D/z_o, computed from the rigorous eqs (18), (21) and (22) (full curves). Simple asymptotic relations shown by the straight dash-dot lines. The circles and dashed lines (detail A) indicate values computed from the fitted relationship which allows calculation of m explicitly in terms of V.

For $V = V_o = 5$, α vanishes, G reduces to 5 and hence $m = 0$, thus satisfying the rigorous equations (18) and/or (21). As V approaches infinity, implying that v is very large or τ_s is very small then

$$G \longrightarrow \frac{2.5}{\gamma_b V} \longrightarrow 0, \quad \text{as } V \longrightarrow \infty \tag{44a}$$

whence

$$m \longrightarrow \gamma_b^2 \, |V| \, V \,, \quad \text{as } V \longrightarrow \infty \tag{43a}$$

which immediately reduces to eq (1) if multiplied by τ_s. Thus the asymptotic behaviour is the same as for the rigorous equations.

Taking V_o equal to 5 and setting $V = 0$ gives the following approximation for m_o, the stress ratio for steady state set-up conditions and zero net flow:

$$m_o \doteq \gamma_b^2 \left[\frac{5}{1 + 10\gamma_b} + \frac{8.85\sqrt{\gamma_b}}{1 + 52\gamma_b^2} \right]^2 \tag{46}$$

where γ_b is given by eq (30). For D/z_o equal to 10^3, 10^4, and 10^5 the corresponding values of m_o computed from eq (45) are respectively 0.097, 0.057 and 0.037 which agree to within one unit in the third decimal place with the values found from the full curves of Fig. 11.

Values of m from the approximate formula (43) (together with (44) and (45)) are compared in Figure 11 with the more exact relations (40a,b) (together with eqs (41a,b)) for a wide range of values of V (circles represent values from approximate equation). The parameter V_o was taken as 5 for each of the r_o values represented in these curves. An enlargement of the graph in the region of very small m is shown in the inset of Fig. 11. This shows that the only appreciable difference between the approximate eq (43) and the exact equations occurs near $V = 5$, which results from the approximation $V_o = 5$ in eqs (44) and (45).

Throughout all of the preceding development we have considered that the x-axis is taken in the direction of τ_s so that the latter is always positive. If we fix the direction of the x-axis independent of τ_s then it can be shown from eq (43) together with (6b) and (16) that

$$\tau_b = \pm \rho \gamma_b^2 \left[v - v^* G(\alpha) \right]^2 \tag{47}$$

the sign of τ_b being consistent with $v - v^*G(\alpha)$, where

$$v^* = \frac{\tau_s/\rho}{\sqrt{|\tau_s|/\rho}} \tag{48}$$

and

$$\alpha = \gamma_b \left[\left(\frac{v}{v^*}\right) - V_o\right] \tag{49}$$

The function $G(\alpha)$ is the same as that defined by eqs (44a,b) and γ_b is given by eq (30) in terms of D/z_o. Note that the parameter v^* has the units of velocity and takes the sign of τ_s.

A plot of τ_b versus v for the case of $D/z_o = 10{,}000$ is shown in Fig. 12 for different values of τ_s (both positive and negative values). The special case $\tau_s = 0$ is the simple quadratic law, eq (1).

For sufficiently small values of v^*/v the above equations approximate to

$$\tau_b = \rho\gamma_b^2 \; |v| \; v - 5\gamma_b \, \tau_s, \text{ for} |\tau_s| < 10^{-4} \rho v^2 \tag{50}$$

Kivisild (1954, p. 83) suggested a similar relation* for the entire range of τ_s; the present theory indicates that this form is applicable to very small values of $\tau_s/\rho v^2$ only; or for a given τ_s eq (50) holds only for large values of v.

SUMMARY

A generalized formula for the bottom shear stress τ_b, exerted by the fluid on the bed of a channel, is derived which takes into account the shear stress τ_s at the surface of the fluid as well as the mean current v in the channel. In addition the dependence of the bed resistance on channel depth and bottom roughness is taken into account. The formula, in sufficiently accurate form, is given by eq (47) together with eqs (30), (48), (49), and (44a,b). In effect the influence of the surface wind stress enters as a correction factor to the usual quadratic law for bottom stress, where the correction term is added or subtracted from the mean current. As can be seen from eq (47) or graphically from Fig. 12,

* In terms of the present symbols, Kivisild suggested the approximation $\tau_b = \rho\gamma_b^2 |v| \; v - m_0\tau_s$. Actually m_0 is much less than $5\gamma_b$.

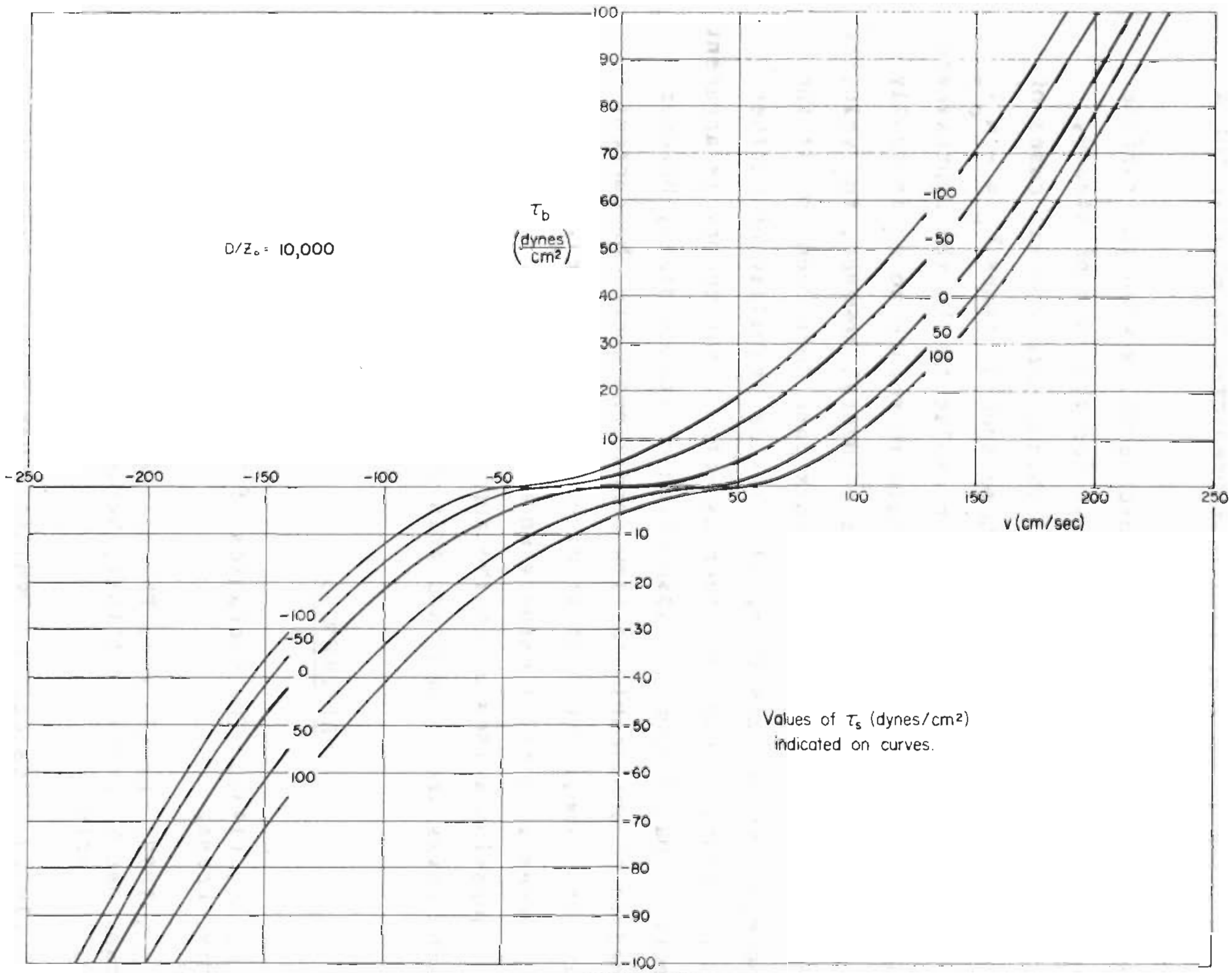

FIGURE 12

Bottom stress versus mean current for five different wind stresses, ranging from -100 dynes/cm^2 (opposing wind) to +100 dynes/cm^2 (following wind), for the case of $D/z_o = 10^4$. Note particularly the pronounced asymmetry of the isoline spacing for opposing wind stress and following wind stress. Also note that the range of bottom stress as delineated by the isolines for τ_s = -100 and +100, increases with the absolute magnitude of the current. (The wind stress of 100 dynes/cm^2 corresponds roughly to a wind speed of the order of 100 knots).

the influence of a following wind (i.e., in the same direction as the current) is to give a bottom stress which is less than that predicted by the simple quadratic formula, eq (1) , while an opposing wind yields a bottom stress which is greater than that predicted by eq (1), for a given value of the mean current v.

The simple quadratic law, eq (1), which applies when the surface stress is negligible, and the bottom stress for the case of steady, wind-induced set-up of water in a bounded channel are special cases of the general formula. In the latter of these special cases $\tau_b = - m_o \tau_s$ where m_o is given implicitly by eq (37) or explicitly by the approximate eq (46). The small amount of empirical data in regard to m_o is really not sufficient to verify this aspect of the theory; however, the velocity distribution predicted by the theory in this case does seem to fit the scatter of observed velocities (Fig. 1). The desirability of further measurements for testing this and other aspects of the theory is apparent.

The theory is based upon the assumption of steady state; however it is presumed to be applicable to flow conditions where the current varies slowly with time, such that it might apply adequately to the case of very long surges in a tidal estuary under the influence of storm winds. Some question arises as to the applicability of the formulas when large wind waves are present and this aspect needs further investigation.

REFERENCES

Bakhmeteff, B. A., (1936) The Mechanics of Turbulent Flow, Princeton Univ. Press.

Boussinesq, J., (1877) Essaisur la Theorie des Eaux Courantes, Mem. Acad. des Sciences de l'Inst. National de France, Tome 23, No. 1, Paris

Brunt, David, (1941) Physical and Dynamical Meteorology, Cambridge Univ. Press.

Dronkers, J. J. and J. C. Schonfeld (1955) Tidal Computations in Shallow Water, Proc. Am. Soc. Civil Eng., Vol. 81, Separate No. 714

Forrsblad, L., (1947) Effects of Wind, Waves, and Currents on Floating Timber, Inst. of Hydraulics, Roy. Inst. of Technology, Bull. No. 7, Stockholm.

Francis, J. R. D., (1953) A Note on the Velocity Distribution and Bottom Stress in a Wind-Driven Water Current System, Jour. of Mar. Res., Vol. 12, No. 1.

Hellstrom, B., (1941) Wind Effects on Lakes and Rivers, Handlingar, Ingeniors Vetenskaps Akademien, Nr. 158 (Stockholm).

Holmgren, S., B. Liljeholm and O. Zachrisson, (1944) Graduation Thesis at the Royal Institute of Technology (unpublished).

Ichiye, Takashi, (1955) A Short Note on the Dissipation of Seiche, Jour. Oceanographical Society of Japan, Vol. 11, No. 3.

Keulegan, G. H., (1951) Wind Tides in Small Closed Channels, Jour. Res. Nat. Bureau of Stds., Vol. 46, No. 5.

Keulegan, G. H., (1938) Laws of Turbulent Flow in Open Channels, Jour. Res. Nat. Bureau of Stds., Research Paper 1151, Vol. 21

Keulegan, G. H., (1953) Hydrodynamic Effects of Gales on Lake Erie, Jour. Res. Nat. Bureau of Stds., Vol. 50, No. 2.

Kivisild, H. R., (1954) Wind Effect on Shallow Bodies of Water With Special Reference to Lake Okeechobee, Trans. Royal Inst. of Tech., Stockholm, Bull. 43.

Montgomery, R. B., (1943) Generalization for Cylinders of Prandtl's Linear Assumption for Mixing Length, Annals N. Y. Academy of Sciences, Vol. 44, Art. 1.

Proudman, J., (1955) The Effect of Friction on a Progressive Wave of Tide and Surge in an Estuary, Proc. Royal Soc., A. Vol. 233.

Rouse, Hunter, (1946) Elementary Mechanics of Fluids, John Wiley and Sons, New York

Saville, T., Jr., (1952) Wind Set-up and Waves in Shallow Water, Beach Erosion Board Tech. Memo. No. 27, June 1952, 36 pp.

APPENDIX A

MEAN CURRENT FOR NEGATIVE m

In order to evaluate the integrals indicated by eq (17) we make use of the relations:

$$\int \alpha \tan^{-1} \alpha d\alpha = \frac{1}{2}(1 + \alpha^2) \tan^{-1} \alpha - \frac{1}{2} \alpha + \text{const.} \quad \text{(A-1)}$$

$$\int \alpha \ln \frac{1 - \alpha}{1 + \alpha} d\alpha = \frac{1}{2} (\alpha^2 - 1) \ln \frac{1 - \alpha}{1 + \alpha} - \alpha + \text{const.} \quad \text{(A-2)}$$

which can readily be verified. If we take

$$\alpha_o = y/B_o, \quad \alpha_1 = y/B_1 \quad \text{(A-3a,b)}$$

and make use of the relation for y as given by (11), it can be shown that the differential $d\zeta$ can be transformed as follows:

$$d\zeta = - \frac{2B_o^2}{1 + |m|} \alpha_o d\alpha_o = - \frac{2B_1^2}{1 + |m|} \alpha_1 d\alpha_1 \quad \text{(A-4a,b)}$$

Substitution of eqs (10a,b), (A-3a,b) and (A-4a,b) in eq (17) renders the latter equation in a form involving the integrals in (A-1) and (A-2) above plus a simpler integral of α alone. The resulting exact integration gives for $m < 0$, after the expense of some algebraic manipulations:

$$V = \frac{2}{k_o'} \left\{ (1 + r_o + r_1) (1 + \sqrt{|m|}) - B_o \left[\tan^{-1} \frac{1}{B_o} + \frac{1}{2} (1 + r_o) \ln \frac{B_o + \sqrt{|m|}}{B_o - \sqrt{|m|}} \right] - \frac{1}{2} r_1 \ln \frac{B_1 + 1}{B_1 - 1} \right\} \quad \text{(A-5)}$$

The terms $(1 + r_o + r_1)$ and $(1 + r_o)$ are very nearly equal to unity and k_o' is very nearly equal to k_o as explained in the text. Using the approximation (13) the last term (in braces) in eq (A-5) has a magnitude very nearly equal to

$$\frac{1}{2} r_1 \ln \frac{4}{(1 + |m|)r_1} \quad \text{(A-6)}$$

For r_1 of the order of 10^{-3} this term is at most ($m = 0$) about .004, in comparison with values of the first term which is of the order of unity. Even with $r_1 = 10^{-2}$ the expression (A-6) is only .030, which is still negligible. Thus eq (A-5) simplifies to the approximate form (18), with sufficient accuracy.

MEAN CURRENT FOR POSITIVE m

Employing the transforms (A-3a,b) and (A-4a,b) with eq (19a) in eq (16) and making use of the identities (A-1) and (A-2) gives the following exact integration for $0 \leq m \leq r_o/1 + r_o$:

$$V = \frac{2}{k_o'} \left\{ (1 + r_o + r_1)(1 - \sqrt{m}) - B_o(1 + r_o) \left[\tan^{-1} \frac{1}{B_o} - \tan^{-1} \frac{\sqrt{m}}{B_o} \right] - \frac{1}{2} r_1 B_1 \left[\ln \frac{B_1 - \sqrt{m}}{B_1 + \sqrt{m}} + \ln \frac{B_1 + 1}{B_1 - 1} \right] \right\} \quad \text{(A-7)}$$

It can be shown that the last term, modified by $r_1 B_1$ is negligible as long as $r_1 < 10^{-2}$. Neglecting this term and taking $(1 + r_o + r_1)$ and $(1 + r_o)$ as unity, eq (A-7) reduces to the approximation (21). Similar approximations are made in deriving eq (22).

APPENDIX B

OTHER FORMULAS FOR m_o

Kivisild (1954) finds two different relations for evaluating m_o. From his eq 4.4.11 we get*

$$m_o = \frac{[\ln(D/z_o) - 1]}{[\ln(D/z_o) - 1.5]} - 1 \; ; \text{ (Curve 2 of Fig. 10)} \qquad \text{(B-1)}$$

and from his eq 4.4.9 we get the following implicit equation for m_o

$$m_o^{3/2} + 1 - m_o^{1/2} (1 + m_o)\ln \frac{m_o D}{z_o(1 + m_o)} = 0 \qquad \text{(B-2)}$$

(Curve 3, of Fig. 10). The first of these relations is derived on the basis of a linear variation of shear stress and a linear variation of mixing length (eqs (3) and (5a) respectively). The second relation however, is based upon a discontinuous stress and mixing length distribution as shown schematically in Figure B-1. The expression (B-1) is in better agreement with the present theory (curve 1 of Fig. 10) as might be expected since a continuously varying stress is employed.

Although the concept of a discontinuity in the stress distribution is physically unsound, it does lead to remarkably good results for flow in pipes. However, in the case of channel flow where the stresses at the top and bottom may differ considerably, there is no assurance that the procedure of employing a discontinuous stress will be adequate.

*Kivisild employs the notation n in place of z_o, and ξ in place of $1 + m_o$.

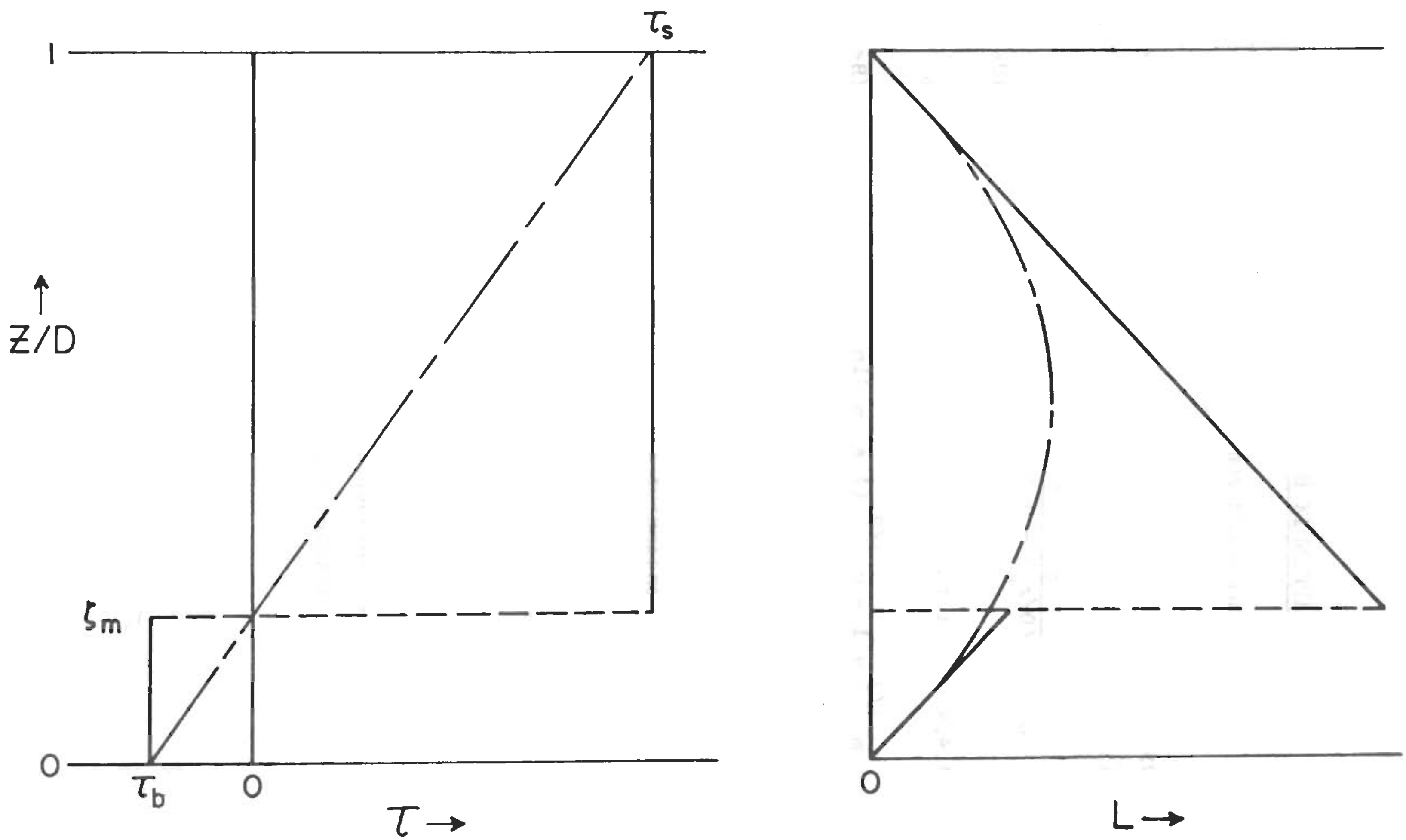

FIGURE B-1

Schematic of stress and mixing length distributions as used in Kivisild's theory (full curves). The distributions used in the present theory shown by dash-dot curves.

APPENDIX C

THE FITTED FORMULA FOR m AS A FUNCTION OF V AND γ_b

Eqs (40a,b) can be expressed in the form

$$m = \pm\gamma_b^{\,2}\,[V - f(m)]^2 \tag{C-1}$$

where the sign is taken consistent with that of the quantity in brackets and

$$f(m) = \begin{cases} f_1(m) & \text{for } m < 0 \\ -f_2(m) & \text{for } m > 0 \end{cases} \tag{C-2}$$

For m = 0 the function f equals $2k_o^{-1}$ which is very nearly equal to V_o. The function f(m) represents a correction term to the simple quadratic formula (42), where the largest value occurs at m = 0, i.e., at $V = V_o$. We wish to be able to express f in terms of V and γ_b rather than m. As a first approximation we might take $m = \pm\gamma_b^{\,2}V^2$ for the purpose of evaluating f(m) in (C-1); this would be a good approximation for large m (hence for large V) positive or negative, but would not be good for small m. A better approximation is to take $m = \pm\gamma_b^{\,2}\,[V - V_o]^2$; this will give the exact value of f at m = 0 and is still a good approximation for very large values of V or m. It will be noted from Figure 11 that if we transform the variable V to $\gamma_b\,(V-V_o)$ this will shift the origin to the existing point of intersection of the curves on the V axis and will produce a (clockwise) rotation of the curves such that they all approach a common asymptote. All these curves are nearly coincident, and if we choose the intermediate curve (that for $r_o = 10^{-4}$) we can evaluate f approximately in terms of the variable $\alpha \equiv \gamma_b\,(V - V_o)$ where we take $V_o = 5$ for simplicity.

For very large m, the asymptotic form of f according to eqs (41a,b) is

$$f(m) \longrightarrow \frac{1}{k_o\sqrt{|m|}} \quad \text{as} \quad |m| \longrightarrow \infty \tag{C-3}$$

and since $\alpha \longrightarrow \sqrt{|m|}$ as $|m| \longrightarrow \infty$ it follows that

$$f \longrightarrow \frac{2.5}{|\alpha|} \qquad \text{as} \qquad |m| \longrightarrow \infty \tag{C-4}$$

where k_o is taken as 0.40.

Consider the function

$$G_o = \frac{5}{1 + 2\,|\alpha|} \tag{C-5}$$

This function has the property of approaching the asymptotic form for f for large α and reduces to 5 at $\alpha = 0$, which is the approximate value of f under this condition. The differences

$$\begin{cases} G_1(\alpha) = f(\alpha) - G_o(\alpha), & \alpha < 0 \\ G_2(\alpha) = f(\alpha) - G_o(\alpha), & \alpha > 0 \end{cases} \tag{C-6}$$

accordingly reduce very nearly to zero at $\alpha = 0$ and approach zero for large α. It is found graphically that the anomaly $G_1(\alpha)$ has a maximum positive value of 1.88 at $\alpha = -0.40$ and $G_2(\alpha)$ has a maximum negative value of -0.85 at $\alpha = 0.12$.

We can get a reasonable fit of the correction terms $G_1(\alpha)$ and $G_2(\alpha)$ by selecting the forms

$$\begin{cases} G_1(\alpha) = \dfrac{a_1\,|\alpha|^n}{b_1 + |\alpha|^p}, & \alpha > 0 \\[2ex] G_2(\alpha) = \dfrac{a_2\alpha}{b_2 + \alpha^p}, & \alpha < 0 \end{cases} \tag{C-7}$$

The asymptotic forms for very large α are accordingly

$$\begin{cases} G_1 \longrightarrow \dfrac{a_1}{b_1\,|\alpha|^{p-n}} & \text{as} \quad |\alpha| \longrightarrow \infty \\[2ex] G_2 \longrightarrow \dfrac{a_2}{b_2\,\alpha^{p-n}} & \text{as} \quad \alpha \longrightarrow \infty \end{cases} \tag{C-8}$$

These correction terms must be of second order compared with the asymptotic expression (C-4); therefore we require that $p-n > 1$. It is found that by plotting the log of $G_1(\alpha)$ and $G_2(\alpha)$ versus the log of α that the slope for large α can be suitably approximated as 3/2 which satisfies the aforementioned condition.

The position of maximum G_1 or G_2 can be shown from eqs (C-7) to be given by

$$\alpha_m^p = \frac{nb}{p - n} \qquad \text{(C-9)}$$

where α_m is the position of maximum G_1 or G_2 where b is taken as b_1 or b_2 respectively. If we choose $p = 2$ and $n = 1/2$ such that $p - n = 3/2$ as indicated above and evaluate the constants a_1, b_1, a_2, b_2 from the condition that the maximum values of G_1 and G_2 are satisfied, it is found that the function f(m) as represented by

$$G(\alpha) = \begin{cases} G_o(\alpha) + G_1(\alpha) & \text{for } \alpha < 0 \\ G_o(\alpha) + G_2(\alpha) & \text{for } \alpha > 0 \end{cases} \qquad \text{(C-10)}$$

is accurate to within about 0.1 for all values of α. This indicates that the estimation of the correction term f in eq (C-1) by means of $G(\alpha)$ is accurate to within two per cent of the maximum value of this term. The resulting formulas for $G(\alpha)$ with the appropriate constants are given by relations (44a,b).